

A FLUIDIC CONTROLLED SEISMIC SOURCE

by

JOHN B. THUREN

ProQuest Number: 10795979

All rights reserved

INFORMATION TO ALL USERS

The quality of this reproduction is dependent upon the quality of the copy submitted.

In the unlikely event that the author did not send a complete manuscript and there are missing pages, these will be noted. Also, if material had to be removed, a note will indicate the deletion.



ProQuest 10795979

Published by ProQuest LLC (2019). Copyright of the Dissertation is held by the Author.

All rights reserved.

This work is protected against unauthorized copying under Title 17, United States Code
Microform Edition © ProQuest LLC.

ProQuest LLC.
789 East Eisenhower Parkway
P.O. Box 1346
Ann Arbor, MI 48106 – 1346

A Thesis submitted to the Faculty and the Board of Trustees of the Colorado School of Mines in partial fulfillment of the requirements for the degree of Doctor of Science in Geophysical Engineering.

Signed: John B. Thuren
John B. Thuren

Golden, Colorado

Date: December 1, 1969

Approved: Frank A. Hadsell
Frank A. Hadsell
Thesis Advisor

John C. Hollister
John C. Hollister
Head of Department

Golden, Colorado

Date: 1 December, 1969

ABSTRACT

A portable fluidic controlled vibrator was constructed and field tested to demonstrate the practicality of employing vibrator sources for near-surface exploration and research.

The vibrator has a power of 2.9 horsepower and a frequency range of 120 to 30 Hz. The input to the ground can consist of either fixed frequencies or a sweep of frequencies. The sweep frequency range can cover any part of the vibrator spectrum, always starting at the high frequency, and ending at the low frequency.

The weight of the vibrator is 150 pounds which makes it portable and its small size allows it to be carried in any vehicle. The power source can be any air compressor capable of achieving a pressure of over 120 psig. Normally the compressor does not run simultaneously with the vibrator therefore the compressor storage tank should have sufficient capacity to supply the vibrator during a run. The air consumption of the vibrator at 200 psig is 154 SCFM. This flow rate should be maintained by the storage tank for the length of the run, which is normally 1/2 second.

The vibrator can be run either vertically or horizontally. Coupling of the vibrator to the ground is accomplished by standing the vibrator on the surface or by partial burial.

The field tests were carried out in three locations in Colorado. One is located near Mead, another is southwest of Denver. Both of these areas are

on the relatively homogeneous Pierre Shale. The third site is on a Paleocene lava flow near Golden. Geophone spreads were laid out up to 240 feet from the source. No difficulty was encountered in transmitting energy to the last geophone.

Records from the Mead site showed Rayleigh waves and body waves. The bedding of Pierre Shale at this location is almost horizontal. The calculated value of Poisson's ratio for the near surface is 0.42. This is close to the values obtained by McDonal in eastern Colorado at a depth of 500 feet. The shear wave immediately below the first layer at Mead has a velocity of 2860 ft/sec. This is 180 ft/sec higher than reported by McDonal for a depth of 500 feet. At the site south of Denver two refractors were detected. The Poisson's ratio for the two top layers is 0.44, whereas for the bottom layer it is 0.39. At the Golden area recorded velocities were substantially higher, evidencing the more solid underlying rock. Two distinct velocity zones were observed with a Poisson's ratio of 0.31 for the lower zone.

Additional tests were made of the vibrator to investigate the possibility of stacking records to attenuate random noise. These tests showed a very high level of reproducibility of vibrator output.

The results of these experiments indicates that the portable pneumatic vibrator is a useful and an inexpensive source of seismic energy. The use of fluidic components add to the simplicity and reliability of the vibrator.

ACKNOWLEDGMENTS

I should like to express my gratitude to the Continental Oil Company for its loan of vital measuring equipment during my graduate studies. Only this generous assistance made the present research project possible.

I am sincerely grateful to the NDEA Fellowship Program for its financial support.

To Professor John C. Hollister goes my appreciation for his continuing interest in vibrator sources and for serving on my doctoral committee. I am grateful to Professor Frank A. Hadsell for acting as advisor on this research project and for his invaluable suggestions and support in obtaining the field data.

I am also indebted to Professor George T. Merideth, Dr. Robert D. Reed and Dr. Leonard Kalal for serving on my doctoral committee. I wish to thank Mr. Jack P. Kintner for his assistance in machining components for the vibrator.

CONTENTS

	<u>Page</u>
ABSTRACT	iii
ACKNOWLEDGMENTS	v
ILLUSTRATIONS	viii
LIST OF SYMBOLS	x
INTRODUCTION	1
PREVIOUS DEVELOPMENTS	4
The "Vibro seis" System	5
THE FLUIDIC CONTROLLED VIBRATOR	8
Design Objectives	11
Design Restrictions	16
ANALYSIS OF PNEUMATIC COMPONENTS	17
Steady State Sizing of Piston-Mass System	17
Steady State Sizing of Plate Valve	26
Detail of Plate Valve	32
ANALYSIS OF FLUIDIC COMPONENTS	39
Vortex Amplifier	39
VIBRATOR SWEEP FREQUENCY AND SELF STARTING MECHANISMS	50
VIBRATOR TIMER	54
ACCESSORY EQUIPMENT	57
FIELD TESTS OF VIBRATOR	59

	<u>Page</u>
CONCLUSIONS	82
REFERENCES	84
APPENDIX A: Supplementary Formulae	A-1
APPENDIX B: Table of Values for Restriction Flow Calculation .	B-1
APPENDIX C: Values of Constant for Sharp-Edged Orifice Flow Calculations	C-1
APPENDIX D: Assembly Drawing of Vibrator	D-1
APPENDIX E: Bibliography	E-1

ILLUSTRATIONS

<u>Figure</u>		<u>Page</u>
1.	Flow diagram for fluidic controlled vibrator	10
2.	Vortex amplifier flow characteristics	12
3.	Model of a vortex valve	14
4.	Piston free body diagram	20
5.	Single-acting actuator	22
6.	Plate valve schematic	33
7.	Top view schematic of sliding plate	34
8.	Detail of plate valve	36
9.	Detail of sliding plate and driving cylinder	37
10.	Detail of vortex amplifier	40
11.	Spouting velocities for air	43
12.	Detail of slide cylinder	45
13.	Sweep mechanism schematic	51
14.	Schematic of timer	55
15.	Ground coupling tests	62
16.	Reproducibility tests	64
17.	Field record Ken-Caryl Unit of the McDannald Ranch	65
18.	Average velocities Ken-Caryl Unit of the McDannald Ranch	67
19.	Time-distance plot for surface and body waves at the Ken-Caryl Unit of the McDannald Ranch	68

<u>Figure</u>		<u>Page</u>
20.	Field record Biddle Farm	74
21.	Average velocities Biddle Farm	75
22.	Time-distance plot for surface and body waves at the Biddle Farm	76
23.	Field record South Table Mountain	78
24.	Average velocities South Table Mountain	79
25.	Time-distance plot for surface and body waves at South Table Mountain	80
C-1	Sharp-edged orifice data	C-1
D-1	Assembly drawing of vibrator	D-1

LIST OF SYMBOLS

A	Geometric area (in. ²)
A _{ud}	Effective area of restriction (in. ²)
C	Restriction discharge coefficient due to vena contracta
c	Phase velocity of Rayleigh wave (ft/sec)
c'	Pneumatic damping coefficient (pf sec/in.)
F	Weight of piston-mass system (pf)
°F	Degree Fahrenheit
f	Friction drag (pf)
g	Acceleration of gravity (386 in./sec ²)
H	Layer thickness (ft)
Hz	Hertz
K	Constant in restriction flow formula (°R ^{1/2} / sec)
K'	Spring constant (pf/ft)
K''	Spring constant (pf/in.)
k	Wave number
k _p	Pneumatic equivalent spring constant (pf/in.)
M	Molecular mass (29.0 for air)
m	Mass (slugs)
ms	Millisecond
N _{ud}	Ratio of actual to sonic restriction flow (function of pressure ratio across restriction)

n	Polytropic exponent
P	Compressional wave
P'	Total pressure (pf/in. ² absolute)
P''	Total pressure (pf/ft ² absolute)
pf	Pounds force
psia	(pf/in. ² absolute)
psig	(pf/in. ² gauge)
R	Gas constant for air (639.6 in./ ^o R) = 144 R' / M g
R'	Universal gas constant (49.7 × 10 ³ ft ² / sec ² ^o R)
^o R	Degree Rankine
r	Radius (in.)
S	Shear wave
S'	Length of arc (in.)
SCFM	Standard cubic feet per minute at 70 ^o F and 14.7 psia
T	Time (seconds)
T'	Total temperature (^o R)
U	Group velocity of Rayleigh wave (ft/sec)
U', u	Velocity (in./sec)
\bar{u}	Dimensionless velocity
V	Wave speed (ft/sec)
V'	Volume (ft ³)
V''	Volume (in. ³)

W_{ud}	Weight flow of air through a restriction (pf/sec)
x	Displacement (in.)
α	Compressional wave speed (ft/sec)
β	Shear wave speed (ft/sec)
γ	Ratio of specific heats (1.4 for air)
Δ	Pressure fluctuations (psi)
ρ	Density
θ	Angle (degrees)
τ	Cylinder charging time constant (sec)
μ	Lame's constant
ω	Angular frequency (rad/sec)

Subscripts

d	Downstream of restriction
i	Intercept
p	Piston
u	Upstream of restriction
1	Layer 1 or chamber 1
2	Layer 2 or chamber 2
3	Layer 3 or chamber 3
4	Chamber 4

INTRODUCTION

The use of multi-frequency vibrators for seismic exploration has a relatively short history. Early electrodynamic vibrators were developed by Howell and others (1940, p.1-14) and Evison (1953, p.4-13). Further development work has been carried out by the Continental Oil Company. These developments consist of a rotating eccentric mass system and a sophisticated electrohydraulic servovalve controlled system (Cherry and Waters, 1968, p.229). In addition to vibrator developments the Continental Oil Company introduced the Vibroseis (Trademark of Continental Oil Company) technique in which a range of frequencies is put into the ground after which input and recorded signals are processed by crosscorrelation (Crawford and others, 1960, p.95).

The developments previously mentioned have brought the use of multi-frequency vibrators to a relatively high state of sophistication, however, it was felt by the author of this paper that there still exists latitude for further vibrator source developments. Specifically, no previous use has been made of compressed air as the power source. In the past pneumatic systems have been second in importance to hydraulic systems for the following reasons: in general they require, filtering and drying of the air supply, some lubrication of moving parts, since, air has negligible

lubricating qualities, precision machining of parts and high air flow rates when the system is quiescent. In addition, the design of pneumatic systems is more difficult because of the effect of the compressibility of air on system performance.

Some of the above mentioned problems or other problems of comparable difficulty exist in hydraulic systems and therefore the gap in relative potential of the systems is not as great as it would at first appear.

In the last few years the field of pneumatics has been greatly improved with the development of fluidic (no moving parts) components. These components depend for their functioning upon interaction between air flows in enclosed passageways. Many different kinds of fluidic devices have been produced. These devices have until quite recently been research laboratory prototypes. Gradual and increasing use is being made of them in engineering applications as their characteristics become better known and more familiar to researchers and engineers.

Due to these advances in pneumatic systems it appeared appropriate to carry out an investigation to determine the feasibility of a fluidic controlled vibrator for seismic use. Some of the looked for advantages would be: reliability due to fewer moving parts, low cost due to easing of precision machining requirements, less maintenance as compared to conventional mechanical valves, insensitivity to operation on contaminated or dust-laden air, and the storage of energy in compressed air.

In order to prove the feasibility of the fluidic controlled vibrator and at the same time provide a tool useful to the Department of Geophysics at the Colorado School of Mines, it was decided to construct a unit small enough to be carried in a jeep type vehicle and be powered by a trailer mounted air compressor.

Engineering applications of seismic techniques often use a hammer blow on the ground for a source. Clearly this method is rather primitive and although seismic records are obtained they cannot be expected to match in any way the sophistication of the Continental Oil Company's "Vibroseis" system.

It is into the gap between hammer sources and the large scale "Vibroseis" system that the fluidic controlled vibrator can make its contributions. Specifically they are light weight, low cost, easily maintained, have frequency sweep capability and are easily powered by compressed air.

PREVIOUS DEVELOPMENTS

The use of seismic energy in the search for oil has a long, distinguished history and a tabulation of previously developed sources is of interest.

Impulse Sources

Weight Drop

Hammer Blow

Explosives

Gas Exploder

Air Gun

Variable Frequency Sources

Electrodynamic Vibrator

Hydraulic Servovalve Vibrator

Some of these sources have been used not only for oil exploration, but, also for near surface engineering applications and research into determining the properties of earth materials.

THE "VIBROSEIS" SYSTEM

To date no completely portable multi-frequency vibrator system exists. This paper reports the design and test of a fluidic controlled pneumatic vibrator. It is anticipated that a portable recording system will be designed and built for use with this vibrator. To emphasize the characteristics of such a system it is useful to outline first some existing techniques which have been developed by Continental Oil Company, that is, the "Vibroiseis" system.

The vibrator with its reproducible output can be run repeatedly to provide stacking of record traces. In addition the vibrator can be run over whatever range of frequencies the earth transmits well. Thus in spite of a vibrator low energy output per run it can provide results equal to that obtained from high energy explosives. This feature is also desirable in areas with a large population density and in noisy surroundings where random noise generation is high.

The multi-frequency vibrator developed in this thesis can be set for either a continuous fixed frequency output or for a changing frequency over a period of time.

Usually single pulse sources emit a relatively narrow spectrum of frequencies, with most of the energy in the region below 50 Hz. High energy in this frequency range can easily excite undesirable modes of propagation. The energy from any source is absorbed as compressional waves,

shear waves and surface waves. Experiments with surface sources gives in general a relative energy content near the source of 8 percent for compressional waves, 28 percent for shear waves and 64 percent for surface waves (Pursey, 1956, p.139-144).

This distribution of elastic energy is of course not fixed and depends upon the earth material and degree of mismatch in coupling the vibrator to the ground. In normal exploration and engineering seismics the refracted and reflected compressional waves are of greatest importance. Here again the vibrator has some advantage over the impulse systems in that high energy surface waves are low in frequency and they can be attenuated by running the vibrator at a frequency above the dominant surface wave frequencies. Surface waves which are not generated do not use up the dynamic range in the recording system.

In near surface engineering seismic work the high energy shear waves will tend to dominate near surface compressional reflections. Here again the operation of the vibrator at a high frequency will diminish the shear wave returns by reducing the energy input to the lower frequency shear modes. The use of high frequency geophones (30 - 90 Hz) will further improve the record.

The complete "Vibroseis" system uses fixed gain recording and the process of correlation to obtain what is essentially a normal seismic record. The "Vibroseis" system vibrator introduces into the ground a band of frequencies. A record is made of this frequency sweep, either from a preprogrammed signal, or a geophone placed on the vibrator or on the ground.

The correlation process (Anstey, 1966 p.55) essentially uses

the duration of the input signal as well as its amplitude to discriminate against noise and unwanted return signals. The process might be described as providing a filter ideally matched to the signal being used. Fundamentally the process involves searching the geophone output for replicas of the input record. The search is carried out by displacing input and output signals by a stepped amount. The degree of similarity at each relative location is assigned a value. A plot of these values yields a correlogram. This crosscorrelogram compresses the long reflected signal into short symmetrical wavelets similar to the conventional seismogram from an impulsive source. Interpretations are then made as in a conventional record.

Containing an elaborate system such as "Vibro seis" in a portable unit appears impractical but some of its desirable features could be retained in a small system.

The stacking of traces to eliminate interference can be readily incorporated. The frequency sweep or fixed frequency operation remains the same. For research applications the vibrator can selectively generate elastic waves of interest to the researcher. An example would be placing the vibrator on its side to create a signal rich in horizontal shear waves. Correlation with a miniature field unit may not be practical and certainly the operation of the vibrator from a preprogrammed signal would be expensive. A geophone next to the vibrator or a pre-filtered pressure trace from the vibrator will give a useable input trace for correlation and the record once obtained can be retained for processing in a central facility.

THE FLUIDIC CONTROLLED VIBRATOR

The impetus given to pneumatics by the development of fluidic components has been remarkable. These components are generally known by the name fluid amplifiers. Many different types of units have been developed to meet specific needs. Of particular interest is the vortex amplifier which has characteristics which make it especially useful in high pressure pneumatic systems.

Fluid amplifiers are basically pneumatic components which depend for their operation on interacting fluid streams. The streams are guided and influenced in many ways by the walls which enclose them. Some of these methods of guiding and influencing fluid streams have been given special names. For example: Coanda effect, impact modulation, focused jet, induction and edgetone effect, vortex formation and others.

Any vibrator must have for operation a moving mass. This mass interacts with its surroundings either by action-reaction or by direct action. Direct action is most useful for a single pulse source, for example the hammer blow. The action-reaction system involves having a moving mass inside a housing and letting the housing rest on the ground. The energy output of this type vibrator depends upon the kinetic energy of the internal moving mass. The mass can be accelerated by rigidly connecting it to a double-acting piston and valving air to alternate sides of the piston.

The system which actuates the valving is amenable to development as a fluidic system. In order to have an efficient system it is necessary that the compressed air used to operate the valving be only a fraction of the compressed air being used to drive the piston-mass system. In other words the fluidic controlling system must have high gain. So far only the basic features of the vibrator unit have been discussed. These basic features are shown in Figure 1.

To obtain high gain in the control system it is necessary to carefully match the fluidic components with a suitable valve type. A survey of existing fluidic components and past applications can be found in Gill and Thuren (1966, p.2-12).

Modern developments in pneumatic valving are discussed in Blackburn and others (1960, p. 214-233).

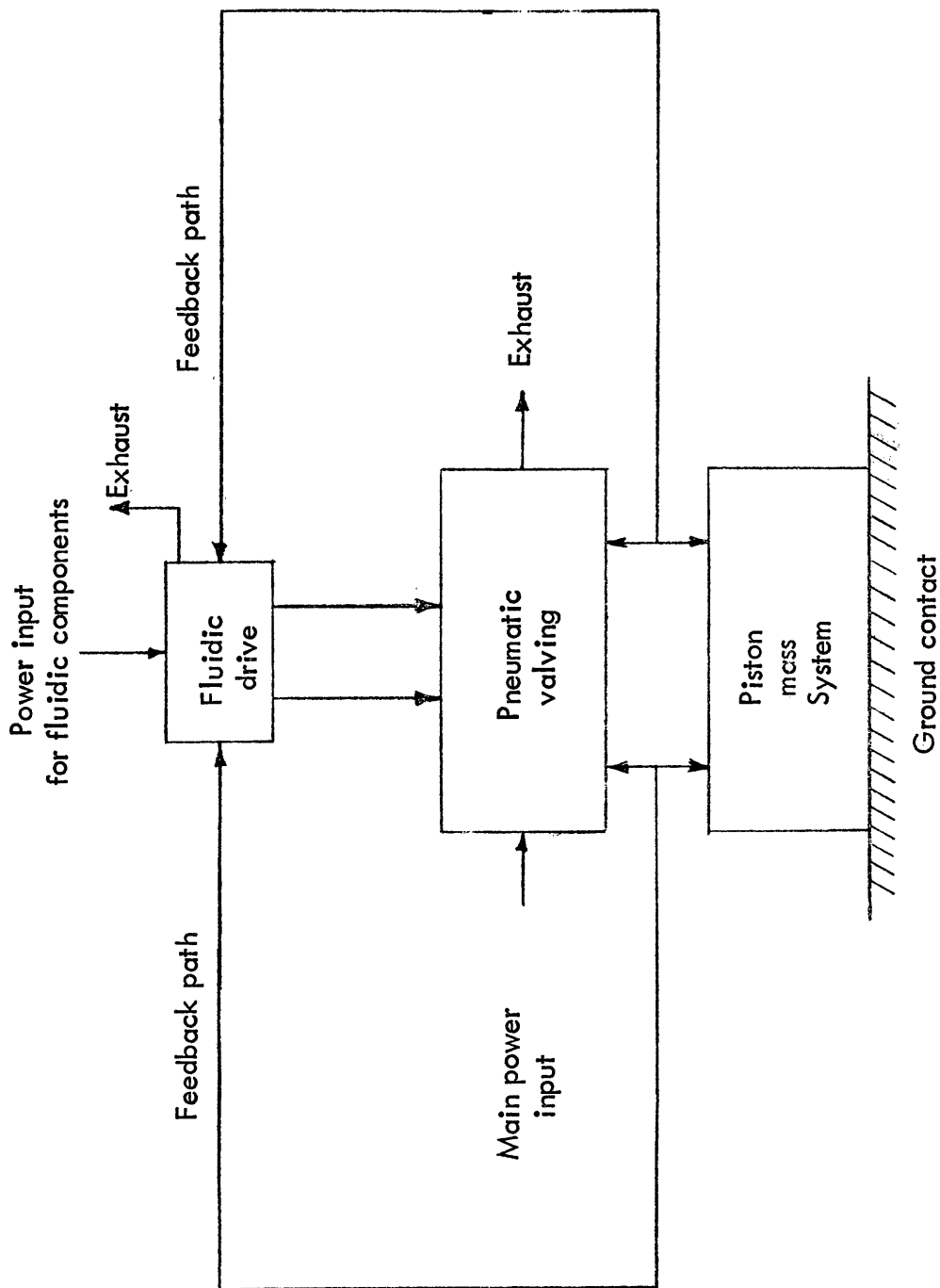


FIGURE 1. Flow diagram for fluidic controlled vibrator.

DESIGN OBJECTIVES

The desire to make the vibrator portable and easily handled is a dominating factor in its design. A weight of 150 pounds would seem to be the upper limit, with a diameter of about one foot and a height of 2 to 3 feet.

As wide a range of frequencies as possible should be engineered into the unit. This requirement is limited by the high gain needed in the control system. A separate oscillator could be designed to operate the valving, but, such an oscillator would require a large air supply of its own thereby reducing the gain. A feed back flow system as shown in Figure 1 appears to be the most efficient system.

The pneumatic valving should be compatible with the long life characteristics of no moving parts fluid amplifiers. The sliding plate valve is perhaps the most rugged of the pneumatic valve types. It has only one moving part, is easy to machine, allows great freedom for design modifications, has a low wear rate because the sliding plate is air cushioned from surrounding parts and it is almost completely force-compensated. The sliding plate valve can be thought of as a piston mass system. The sliding plate must be driven from an external source. In this case the drive will be a vortex amplifier. A schematic diagram of this device is shown in Figure 2.

The vortex amplifier is really a combination of a vortex valve and an external flow pickoff. A vortex valve with a graph of its flow and pressure characteristics is

Pickoff flow characteristics

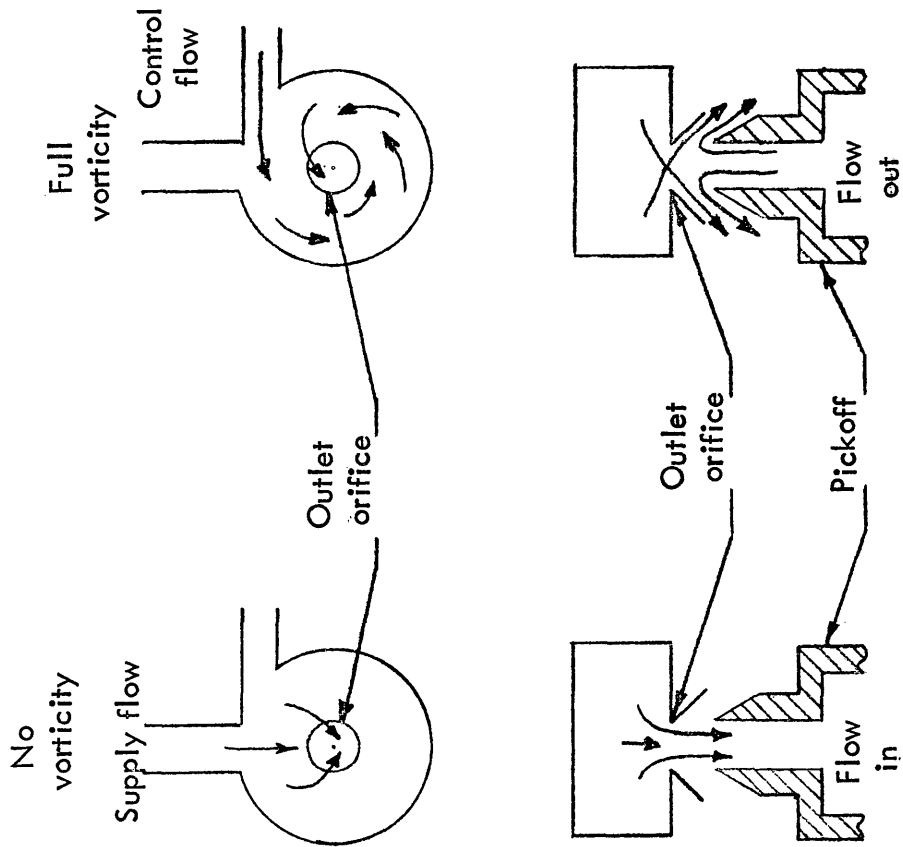
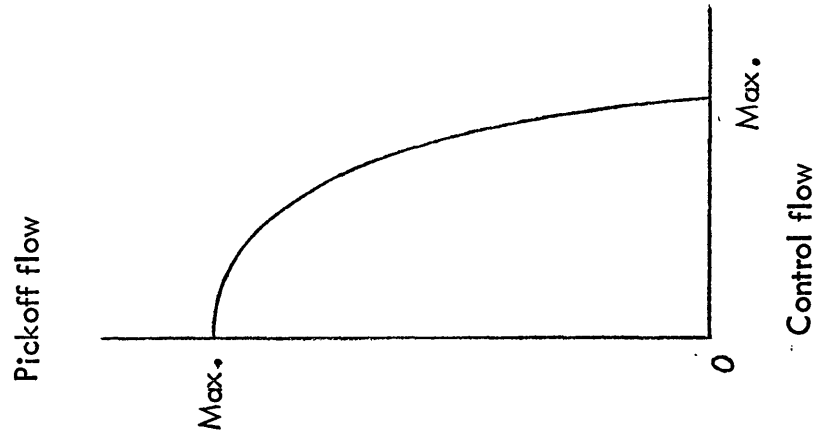


FIGURE 2. Vortex amplifier.

illustrated in Figure 3. The vortex valve acts as a variable flow restrictor when connected in a fluidic circuit. With the control inlet closed the supply flow goes directly through the valve and maximum flow depends upon the inlet or outlet restriction whichever is the smallest. Introduction of a control flow tangentially into the spin chamber causes formation of a vortex, which in turn shears off the entering supply flow forcing it to spiral inward to the outlet. A plot of turndown ratio is shown on graph of Figure 3. The vortex valve is completely shut off when total flow through the valve is equal to the maximum control flow. This effect of vortex formation can be combined with a flow pickoff to form a vortex amplifier. With just supply flow admitted to the spin chamber, no vortex is formed and the flow exits from the spin chamber as a circular jet. By correctly locating and dimensioning the pickoff, the jet from the valve exit will be captured by the pickoff. Increasing the control flow from zero increases the vorticity and the exit jet is changed into a cone shaped annular jet. The angle of spread of the jet is regulated by the control flow and therefore the amount of flow into the pickoff. A graph of control flow versus pickoff flow for a typical vortex amplifier is shown in Figure 2. The most important feature of Figure 2 is that the pickoff flow goes completely to zero at high vorticity. This feature allows a reverse flow in the pickoff. If the sliding plate is to be driven as a piston-mass system the piston cylinder must be scavenged during part of the cycle. No other fluid amplifier component exhibits this feature to the same degree as the vortex amplifier.

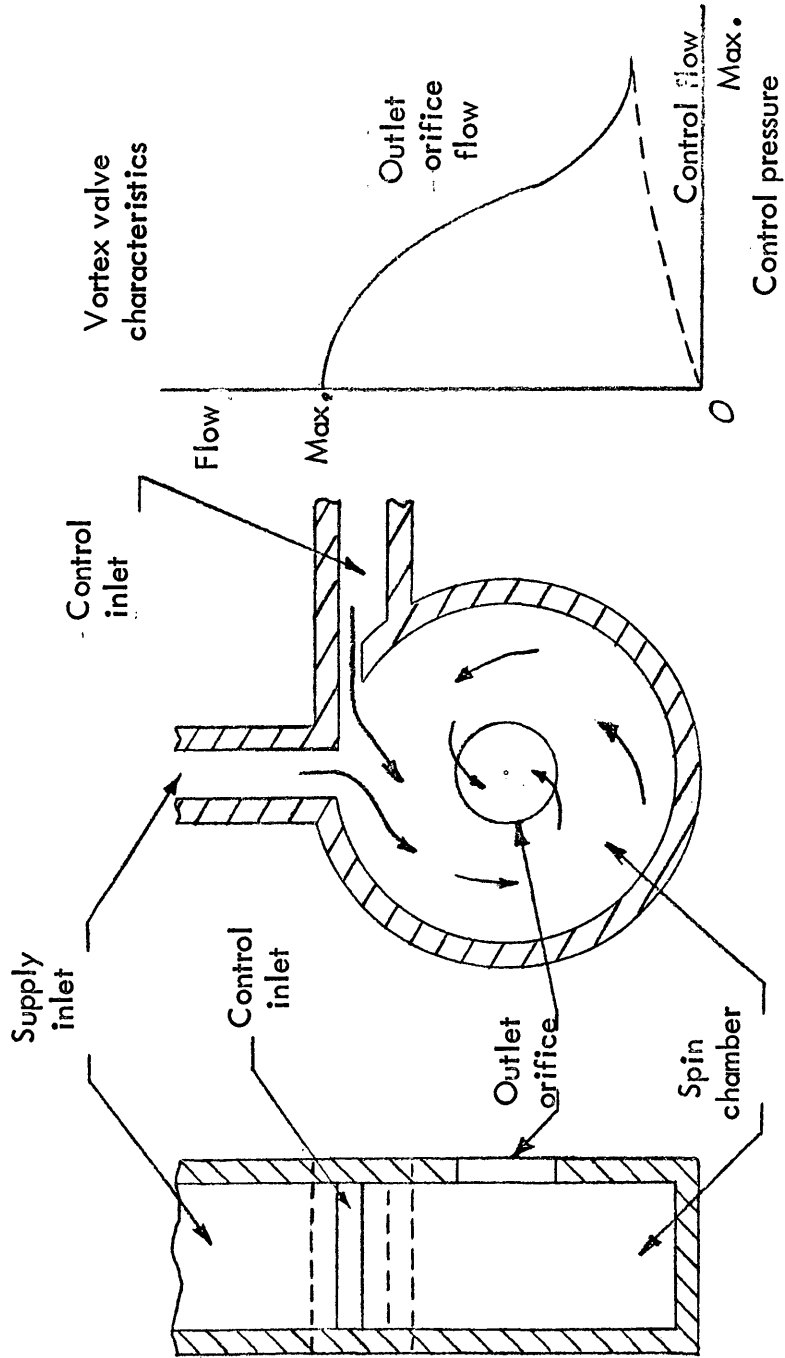


FIGURE 3. Model of a vortex valve.

The control inlet of the vortex amplifier can be connected via a feedback line to the exhaust from the pistonmass system. This type of feedback loop is commonly called a closed loop system. It allows a very high gain, its main drawback is that the maximum attainable cyclic rate is determined by the shortest possible feedback path. In pneumatic systems the transmission of a pulse down a tube is limited to the local speed of sound.

Anticipating a weight for the piston-mass system of 10-20 pounds and a weight for the sliding plate of 1/10 pound a gain of 100 to 200 could be expected for this design.

DESIGN RESTRICTIONS

As previously mentioned the feedback path limits the maximum frequency of the vibrator. In general maximum flow rate occurs in enclosed channels when the pressure ratio across the ends of the channel is about 0.53. This effect is due to the compressibility of the air. Well established formulae exist for calculation of air flow through orifices. These calculational procedures are stated in Appendix 'A'.

Some provision must be made for adjusting the length of time during which the vibrator will run. Fluidic timers exist but at the present state-of-the-art they are too expensive to compete with an electric timing unit. Such a unit was constructed to operate the vibrator. It requires a separate source of electric energy such as can be provided from an automobile battery.

ANALYSIS OF PNEUMATIC COMPONENTS
STEADY STATE SIZING OF PISTON-MASS SYSTEM

There are 3 basic factors which determine the sizing of the portable vibrator. The maximum weight has already been discussed. The others are rate of air consumption and the stiffness of springs required to center the mass and support it against the pull of gravity.

The source of air intended for use with this source was a drilling truck mounted air compressor. Since it was not intended to operate the compressor while running the vibrator, the length of run is limited by the air capacity of the storage tank. The maximum pressure available from this source is 108 psig. This pressure proved to be inadequate to run the vibrator at frequencies above 60 Hz. For these frequencies the minimum supply pressure should be 120 psig. Operation of the vibrator at pressures up to 200 psig has been investigated. No increase in frequency occurs above 120 psig although the energy output increases significantly.

The lack of increase in frequency above 120 psig is attributed to the choking of the feedback lines by the already mentioned compressibility of air.

The stiffness of centering springs must be chosen to properly locate the mass. The springs are limited in their motion by the coils coming in contact with each other. In addition the springs determine the piston cylinder size since the maximum air pressure

available must be able to compress them completely. The maximum movement of the piston determines in turn the fill volume of the cylinder. This in turn must be related back to the air storage tank capacity and length of run desired.

Needless to say, many combinations must be tried before a satisfactory one is discovered.

The following calculations will be carried out for the final combination decided upon.

The square wire compression springs were obtained from *McMaster-Carr Supply Company, Chicago*. Each spring has the following specifications :

Works over rod	1/4 in.
Works in hole	7/16 in.
Free length	3 - 1/2 in.
Wire size	1/16 in.
Solid height	2-3/16 in.
Load per inch	27 pf.

These springs are installed in a special housing as shown in the assembly drawing of the vibrator. The springs are indirectly connected to the mass. The housing is arranged so that the springs are compressed regardless of the motion of the mass each side of center. Two springs act on the mass so that the spring constant is 54 pf/in.

For dynamic operating conditions the springs should not be compressed more than one half the distance between free length and solid height. This distance is 3/5 inch. The reason for this limitation is the increased failure rate due to fatigue when the springs are compressed excessively.

Maximum movement of the mass will occur at the lowest frequency of operation. This was chosen to be 40 Hz.

Figure 4 gives the free-body diagram for the mass. Combining the forces on the piston gives :

$$(P'_2 - P'_3) A_p = F + f + c'u + K''x$$

Where :

P'_2, P'_3 are pressure (psia).

A_p is area of piston (in.²)

F is weight of piston-mass (pf).

f is friction drag of piston rings and cylinder end seals (pf).

u is velocity (in./sec).

c' is pneumatic damping coefficient (pf sec/in.).

K'' is spring constant (pf/in.).

x is displacement (in.).

The weight for the piston-mass system is chosen to be 13.5 pf. and $A_p = 1.0 \text{ in.}^2$. This piston area is obtained by letting the piston cylinder be 1.5 in. in

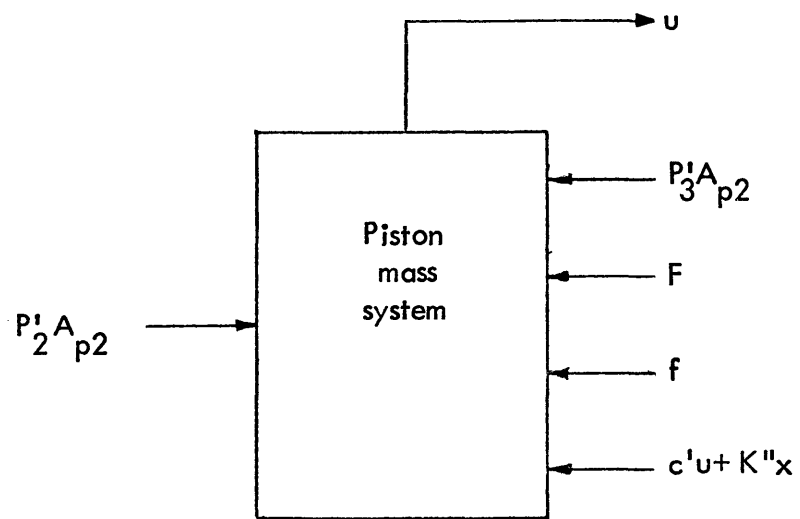


FIGURE 4. Piston free body diagram.

diameter and the piston shaft diameter 1.0 in. in diameter. The frictional drag for a system such as this with rubber seals and rings is about 10 pf.

It will be assumed that the scavenging of the exhaust side of the piston is very efficient and that as a consequence P'_3 can be equated to ambient pressure. This allows simplification of the force equation and permits analysis of the piston-mass system as a single acting actuator. This type of actuator is illustrated in Figure 5.

It is the object of this analysis to determine P'_2 given all terms of the force equation except for the pneumatic damping term. This term is a measure of the energy absorbed by the air in the cylinder. This damping rate is frequency dependent. Values for the damping coefficient have been obtained by experiment (Townsend, 1965) and described mathematically (Anderson, 1967, p. 165). For relatively high frequencies, that is, high in pneumatic systems, the damping coefficient can be approximated by the equation.

$$c' = \frac{k_p \gamma}{(\omega \tau)^2}$$

Where :

$$k_p = n P'_2 A_p^2 / V''_2$$

n is the polytropic exponent

V''_2 is cylinder volume (in.³).

$$\gamma = V''_2 (\Delta P'_2)^{1/2} / 1.198 n \sqrt{2g RT'} A_{23} \sqrt{P'_2}$$

$\Delta P'_2$ fluctuations of P'_2 about equilibrium (psi).

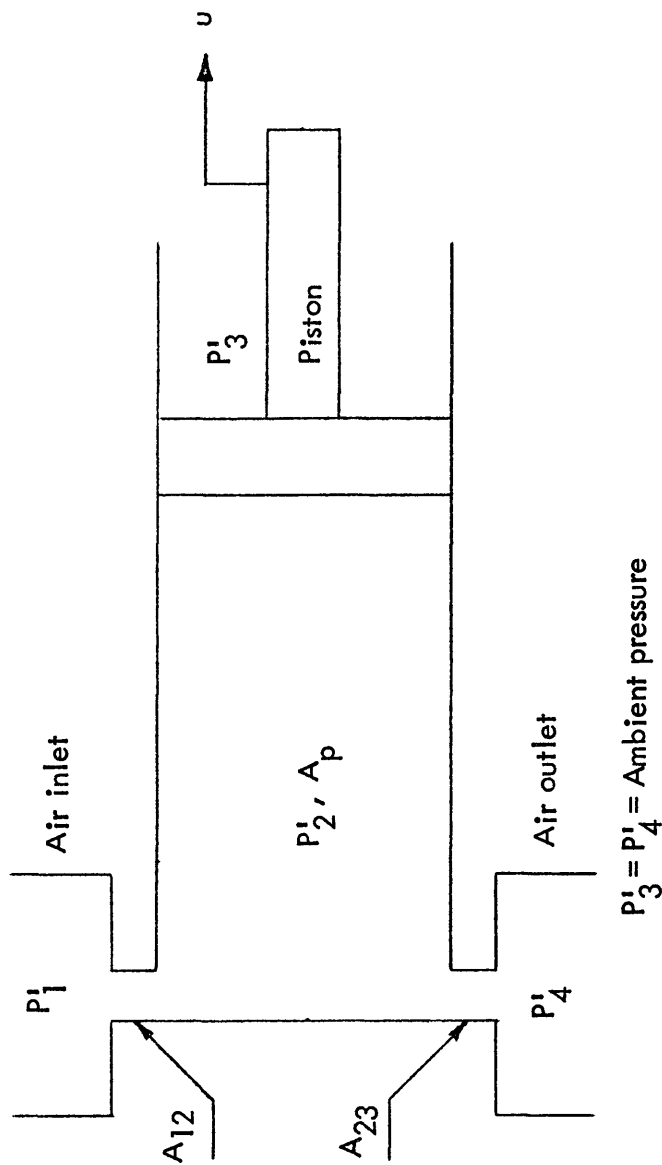


FIGURE 5 • Single-acting actuator •

$P_3^i = P_4^i =$ Ambient pressure

A_{23} is leakage area of cylinder (in.²).

ω is angular frequency of mass (rad/sec).

Direct evaluation of c' from the above equation is impossible. The values of P_2^i , ΔP_2^i , A_{23} and V_2'' are not known. By anticipating that 75 psia may be an acceptable value for P_2^i it is possible to estimate a volume of 1 in.³, since the piston will be statically deflected approximately 1 in. for a pressure of 75 psia. A_{23} and ΔP_2^i remain unknown and further progress can only be made by use of an artifice. The experimental values of c' are at a maximum when $\omega\Upsilon$ has a value of 0.75 rad. This value of ω corresponds to the natural frequency of oscillation. In this case $\omega = \sqrt{K'/m} = \sqrt{(684 \text{ pf/ft})/0.42 \text{ slug}} = 40.5 \text{ rad/sec}$.

Solving for Υ

$$\Upsilon = \frac{0.75}{\omega} = \frac{0.75}{40.5} = 0.0185 \text{ sec}$$

and

$$k_p = \frac{n P_2^i A_2^2}{V_2''} = \frac{(1.4) (75) (1)^2}{(1)^3} = 105 \text{ pf/in.}$$

Note: The polytropic exponent takes values between 1 for a constant temperature process and γ for a constant entropy process. For the high frequencies of the vibrator the process approximates reversible adiabatic. Entropy is constant and therefore $n = \gamma = 1.4$ for air.

Calculating c' with $\omega = 251 \text{ rad/sec}$ corresponding to a frequency of 40 Hz yields

$$c' = k_p \Upsilon / (\omega \Upsilon)^2 = 0.091 \text{ pf sec / in.}$$

To evaluate P_2^1 only u remains to be determined. Maxima of amplitude and frequency are $3/5$ in. and 40 Hz respectively. Hence

$$\begin{aligned} \text{Average Velocity} &= \frac{\text{Distance traveled per cycle}}{\text{Period}} \\ &= \frac{2.4 \text{ in.}}{0.025 \text{ sec}} = 96 \text{ in./sec} \end{aligned}$$

In order to apply the calculated value of c' to the force equation it is first necessary to determine the piston-mass velocity at $x = 0$. This corresponds to the maximum velocity attained at 40 Hz.

The maximum velocity can be calculated in two ways. First by considering the system as being represented by the single-acting actuator. In this case the mass undergoes constant acceleration and the maximum velocity is simply twice the average velocity.

$$\text{Maximum velocity} = 192 \text{ in./sec}$$

The second value can be obtained by considering the system as a harmonic oscillator. Here the maximum velocity is $2/\sqrt{2}$ times the RMS velocity.

For low frequencies (40 Hz) the constant acceleration value is more nearly correct since the return springs have less effect on the system. At higher frequencies (120 Hz) the amplitude of motion diminishes and approaches sinusoidal motion making the harmonic calculation the correct one.

In the equations that follow the value of 192 in./sec will be used, since, sizing of the plate valve is done at 40 Hz and this will give a

safety factor for inevitable pressure losses which will occur as the air passes through the vibrator.

Calculating P_2^i at $x = 0$

$$\begin{aligned} P_2^i &= (F + f + c'u) / A_p \\ &= 13.5 + 10 + (0.091)(192) = 41 \text{ psig} \end{aligned}$$

P_2^i represents the maximum pressure that must be obtained in the cylinder to achieve oscillation at 40 Hz.

STEADY-STATE SIZING OF PLATE VALVE

The requirement of high gain necessitates that some type of pneumatic valve be placed between the fluidic components and the piston cylinder. Many types of valves are available. The choice in this case depends upon the need for reliability and freedom from close tolerances in machining. The plate valve is ideal for this purpose. The plate valve which forms the basis for this application is described in Blackburn and others (1960, p. 230) Several significant modifications have been made to the basic plate valve design for this application. They will be described in this section.

In the preceding section a value of 56 psia was derived for the pressure to drive the vibrator at 40 Hz. The critical sizing of the plate valve will be determined using this pressure. Initially an orifice size will be calculated and then a valve will be chosen and sized to give an effective area of inlet equivalent to the orifice.

In addition to the calculated downstream pressure an estimate must be made of the upstream pressure to be used. The minimum pressure selected is 70 psia. This gives a pressure drop across the valve of 14 psi. Using this low operating pressure for calculating the orifice size will ensure a nominal range of pressure over which the vibrator can operate.

Let P'_1 be the pressure upstream of the plate valve, that is 70 psia. P'_2 is required to be 56 psia. The pressure ratio across the plate valve will be $P'_2/P'_1 = 0.8$. This pressure ratio will be thought of as occurring across a square-edged circular orifice.

The flow through this orifice can be calculated from the equation :

$$W_{ud} = \frac{K P'_u A_{ud} N_{ud}}{\sqrt{T'_u}}$$

This equation is described in Appendix A .

The value for the effective area A_{12} can be obtained by again considering the piston-mass system as a single-acting actuator.

If we assume that the velocity of translation of the actuator is constant then the difference in weight flow is a constant also. That is, the inlet flow W_{12} through the effective inlet area A_{12} minus the leakage flow W_{24} through the effective leakage area A_{24} is a constant. If this air is added to the cylinder at constant pressure then :

$$W_{12} - W_{24} = \frac{P'_2 A_{p2} u_2}{R T'_2}$$

Where A_{p2} is cylinder area.

The flow rates are then equated to the orifice flow equations.

$$\frac{K P'_1 A_{12} N_{12}}{\sqrt{T'_1}} - \frac{K P'_2 A_{24} N_{24}}{\sqrt{T'_2}} = \frac{P'_2 A_{p2} u_2}{R T'_2}$$

This nonlinear relationship can be further simplified and put into useful form by assuming that no substantial change in temperature takes place.

$$A_{12} C_{12} - A_{24} N_{24} = \frac{A_p^2 u^2}{K_R \sqrt{T^2}}$$

Where

$$C_{12} = P'_1 N_{12} / P'_2.$$

At this point some estimate must be made of the leakage effective area as compared to the inlet effective area.

Many past designs of pneumatic systems, particularly those which operate continuously, have been arranged to minimize leakage flow. In these systems leakage is usually kept to 10 percent or less of the inlet flow. In the seismic vibrator, leakage flow is also undesirable but the requirements of easy machinability and reliability are thought to be paramount. The plate valve slide is the only moving part in the control system and it is the part most susceptible to wear and stoppages from water and dirt in the air supply. The slide valve is cushioned by air on all sides and this air flow is a substantial part of the leakage flow. Estimating this leakage flow, especially under dynamic operating conditions, is impractical with the equipment at hand. Hence, the allowance for leakage will be made more than that encountered in conventional pneumatic systems. In this case it is 50 percent. It will be shown in a later section that this value is too large but not unreasonable for calculational purposes. Additional benefits derived by a greater leakage rate, are an increase in stability and response to the driving forces.

The dimensionless velocity \bar{u}_2 can now be written in terms of C_{12} and N_{24} .

$$\bar{u}_2 = \frac{A_{p2} u_2}{KR \sqrt{T'_2} A_{12}} = (C_{12} - 0.5 N_{24})$$

Values for N_{ud} are tabulated in Appendix C .

$$C_{12} = \frac{P'_1 N_{12}}{P'_2} = \frac{70 (0.82)}{56} = 1.02$$

$$N_{24} = 1.0$$

$$\frac{A_{p2} u_2}{KR \sqrt{T'_2} A_{12}} = 0.502$$

Before it is possible to calculate the effective inlet area A_{12} the temperature of the supply air must be known. Tests were made on the drilling truck compressor. Under intermittent usage with the compressor thoroughly warmed up the air temperature was approximately 150 °F with the ambient temperature 30 °F. It is clear that on a warm day the compressor air temperature would be somewhat higher, but it would probably never exceed 175 °F. To proceed with the calculation of A_{12} the 150 °F figure will be used.

$$A_{12} = \frac{A_{p2} u_2}{KR \sqrt{T'_2} (0.502)} = \frac{(1)^2 (192)}{(0.532) (639.6) \sqrt{(610)} (0.502)} = 0.0455 \text{ in.}^2$$

The rate of flow through A_{12} at these pressure and temperature conditions can now be obtained.

$$W_{12} = \frac{K P_1 A_{12} N_{12}}{\sqrt{T_2}} = \frac{(0.532)(70)(0.0455)(0.819)}{\sqrt{610}} = 0.0564 \text{ pf/sec}$$

At an inlet pressure of 135 psia, corresponding to the minimum pressure necessary to operate the vibrator at 120 Hz, the flow rate can be calculated in the same way.

$$W_{12} = \frac{(0.532)(135)(0.0455)(1)}{\sqrt{610}} = 0.132 \text{ pf/sec} \equiv 106 \text{ SCFM}$$

Note : The unit SCFM used above is described in the list of symbols.

The rate of flow at 135 psia is approximately twice the flow rate at 70 psia. These figures can now be compared with the air capacity of the drilling truck storage tank. The volume of the tank is 4.05 ft³. For stable operation of the vibrator during a run the allowable pressure variation in the tank will be restricted to 10 psi. A wider range of available flow rates can be obtained from the same tank by compressing the air to a pressure considerably above the needed pressure and then placing a pressure regulator in the air supply line to the vibrator. No further consideration will be given to the regulator, since, the vibrator has proved to be quite insensitive to pressure changes provided the minimum pressure is kept above 135 psia.

Applying the general gas law in Appendix A to a tank with volume 4.05 ft³ and pressure 145 psia yields for the mass in the tank.

$$m = \frac{P V M}{R T} = \frac{(20.9 \times 10^3)(4.05)(29)}{(49.7 \times 10^3)(610)} = 8.1 \times 10^{-2} \text{ slug}$$

For a pressure of 135 psia the mass is 7.53×10^{-2} slug. The mass difference between these pressures is 0.57×10^{-2} slug. If this amount of air is discharged in one second the flow rate will be 145.5 SCFM. Normally the vibrator will be run for one-half second to two seconds depending on the recording system being used with the vibrator. In addition the orifice flow rate calculated (106 SCFM) is the maximum flow rate and the flow rate average over a cycle will be less. It is therefore concluded that the drilling truck tank is large enough to power the vibrator.

The effective orifice size that has been calculated is not the geometric area of the orifice. This is because of the vena contracta effect (Streeter, 1962, p. 222) encountered any time a flow is forced through a change in area in the flow passage.

Considerable experimentation has been carried out to determine the relationship between effective area and geometric area depending upon the geometry of the orifice. For the square edged orifice the relationship is expressed sufficiently accurately by the following equation.

$$\text{Geometric area} = \text{Effective area} / 0.82$$

This equation is valid for a wide range of pressure ratios. This is not true for the sharp-edged beveled orifice, which will be discussed later. A plot of coefficients for this type orifice is shown in Appendix C.

DETAIL OF PLATE VALVE

The required area of the plate valve orifice is calculated to be 0.055 in.^2 . This area must now be related to the opening in a plate valve. A plate valve schematic is drawn as Figure 6. A top view schematic of the sliding plate is illustrated in Figure 7.

From Figures 6 and 7 it can be seen that the opening uncovered in the plate valve by the sliding plate is in the shape of two equal circular arcs bounded by two parallel straight lines. Although the maximum required area is known to be 0.055 in.^2 the length of the opening must be coordinated with a width of opening that can be achieved by the vortex amplifier driving the sliding plate. As shown in Figure 6 the air passes on both sides of the slide. This feature is of vital importance otherwise the slide would be forced against one side of the valve body with great force causing it to jam. Another desirable advantage of this feature is that it reduces the degree of movement required of the slide by doubling the opening area. The compressibility of the air requires that one more criteria be kept in mind when designing the plate valve. This is that the air being exhausted to atmosphere expands and requires larger porting to properly scavenge the exhaust side of the cylinder. The previous calculations were based upon having P'_3 equal to ambient pressure. While it is impossible to achieve this low a pressure at the high frequency of operation, it can be approached by making the exhaust port at least twice the area of the inlet port. In the final valve design this feature is accomplished by constructing a bridge between the ports as shown

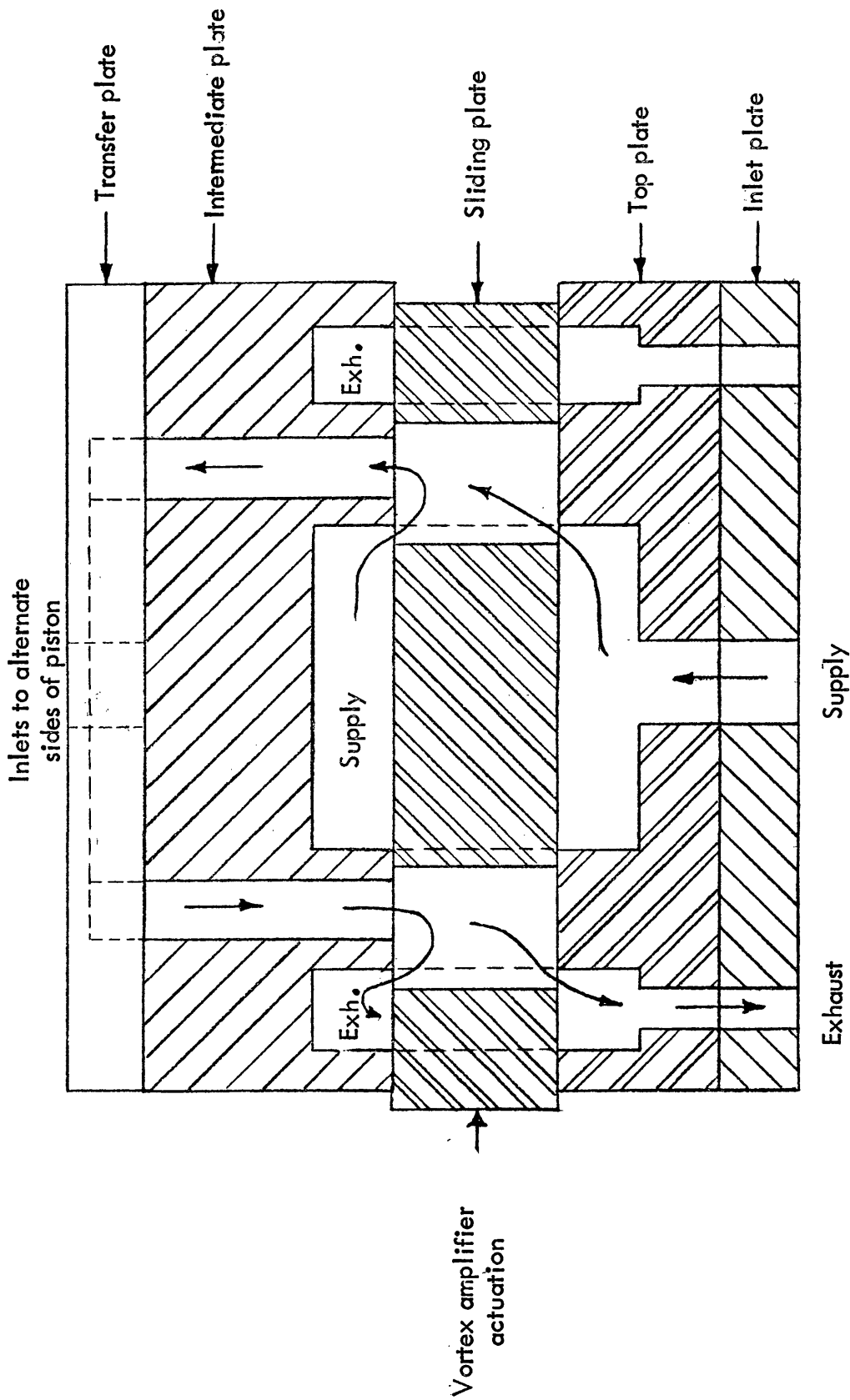


FIGURE 6. Plate valve schematic.

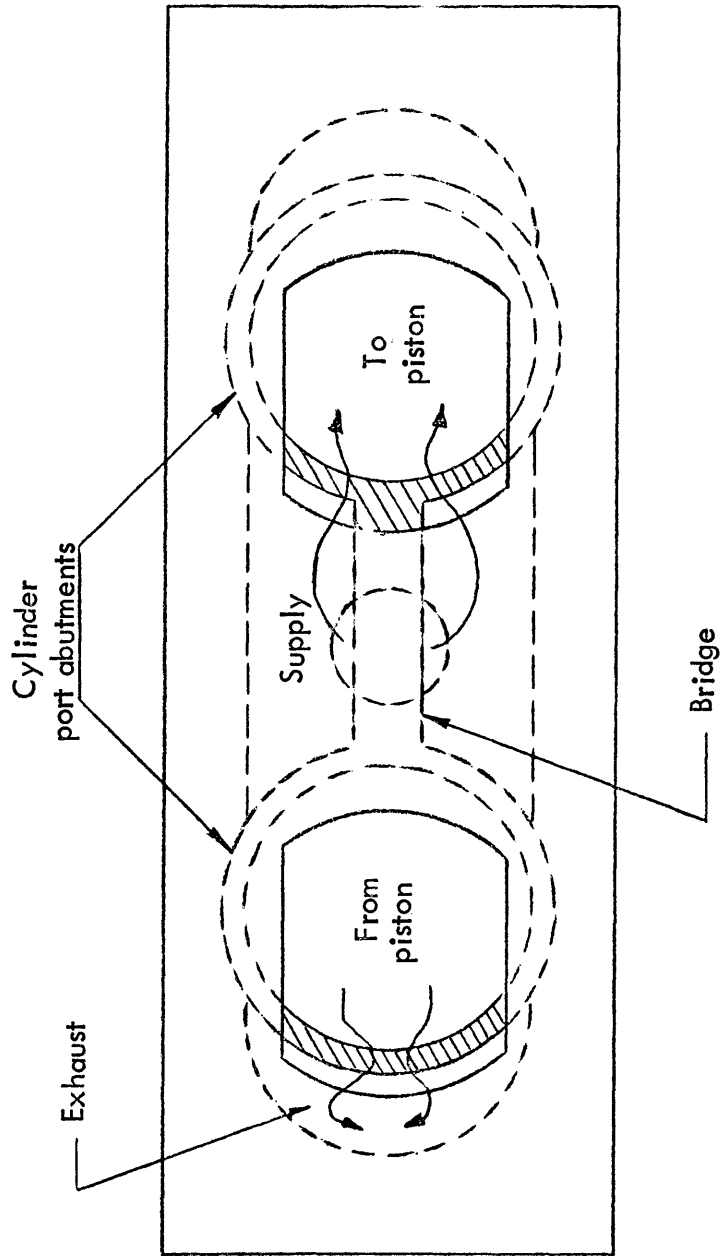


FIGURE 7. Top view schematic of sliding plate.

in Figure 7. The width of the bridge determines the relationship between inlet and outlet areas. The needed area for the exhaust port becomes 0.11 in.^2 . The size finally chosen to fit the requirements was a cylinder port abutment diameter of 1.0 in. The length of the slide slots are cut to 0.998 in. to overlap the abutments 0.001 in. on each end when the slide is centered. This overlap reduces the leakage flow in the centered position and the overlap is small enough to preclude development of a dead spot in the piston driving cycle. This detail is laid out in the machine drawings of the plate valve (Figures 8 and 9). The slide slots have been made 0.75 in. wide. This width subtends an angle on a one inch circle of 97 degrees when it intersects the circle. The length of arc corresponding to this angle is readily calculated.

$$S' = \pi r \theta / 180^\circ = 0.845 \text{ in.}$$

Dividing this arc length into the area will give an estimate of the required slide movement.

$$A/S' = 0.055/0.845 = 0.0651 \text{ in.}$$

Total peak to peak movement must be at least 0.13 in. This amplitude can be readily achieved by the vortex amplifier.

Specific arrangement of the inlet and exhaust channels can be seen on the machine drawings. It will be noticed that two diagonal channels are milled into the intermediate plate. These are necessary because the direction of motion of the slide is

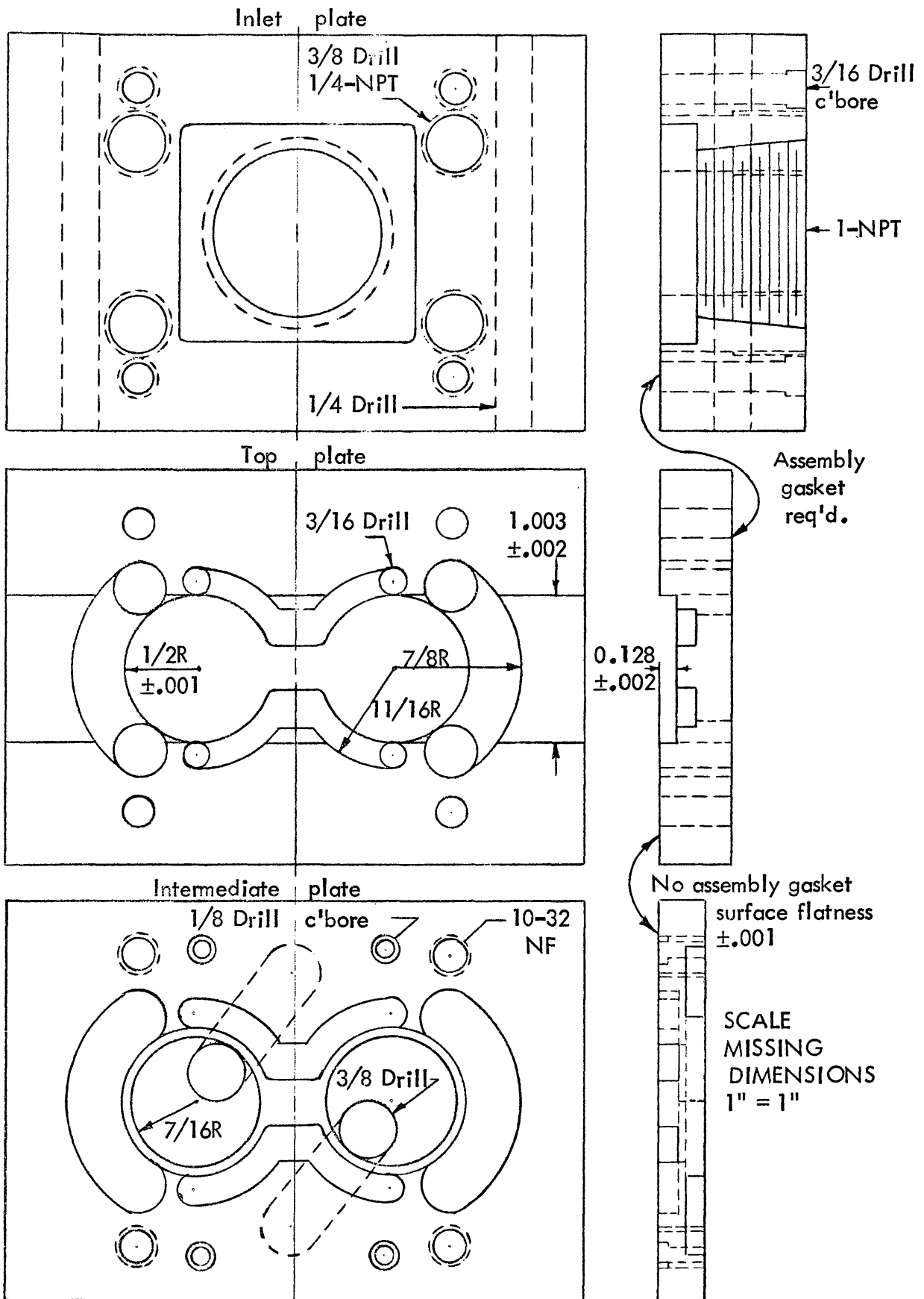
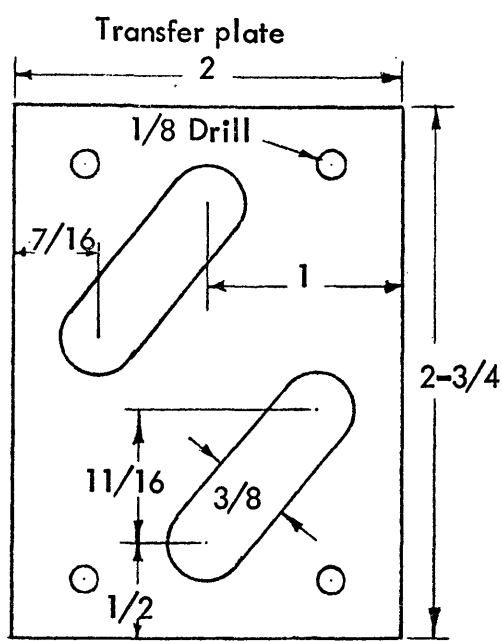
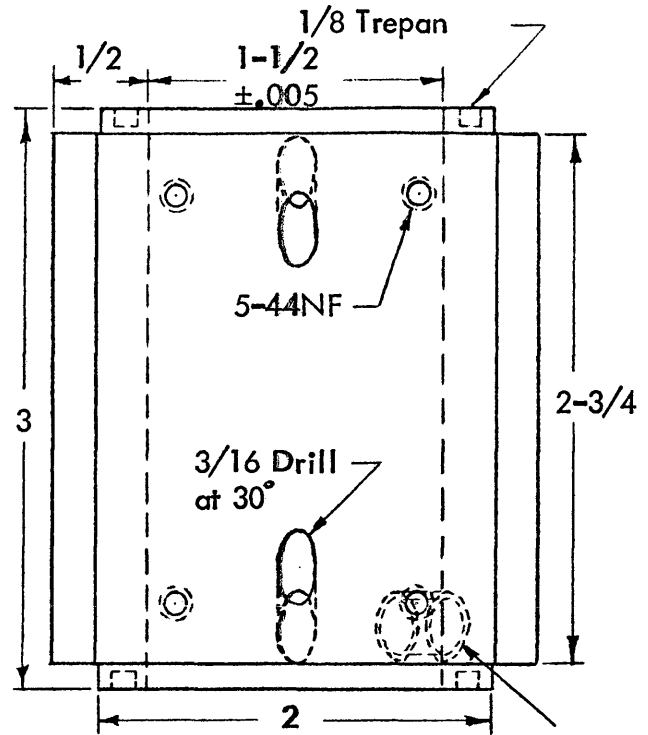


FIGURE 8. Detail of plate valve.

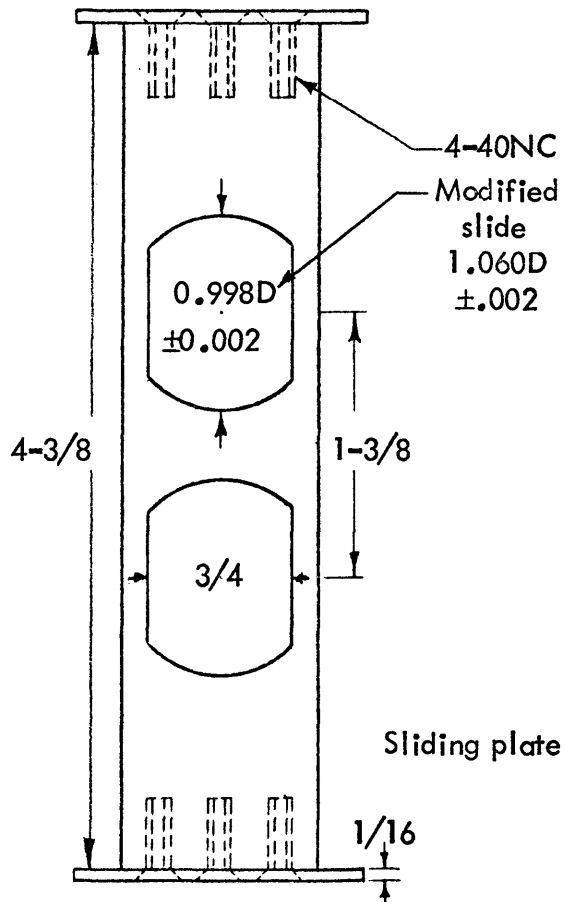


Assemble between intermediate plate and driving cylinder. Gasket both sides. Thickness of plate 1/8



Driving cylinder

1/8-NPT
For pressure transducer



Sliding plate

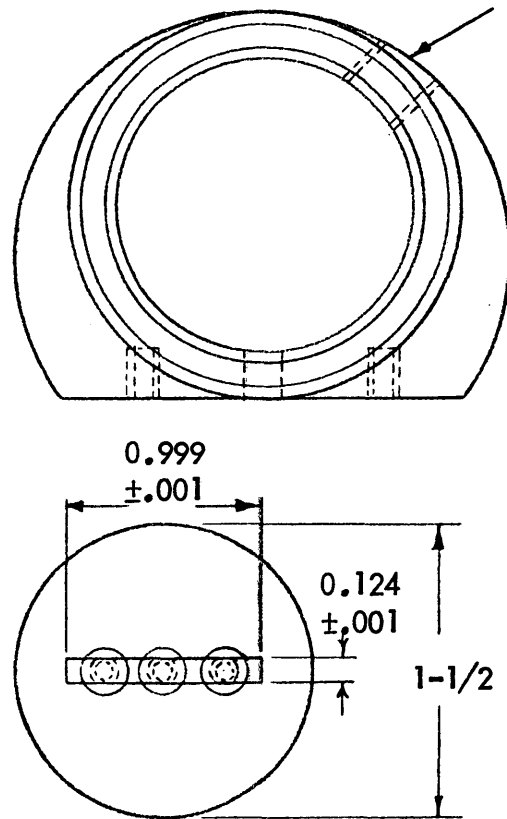


FIGURE 9. Detail of sliding plate and driving cylinder.

perpendicular to the motion of the piston-mass. This arrangement prevents the motion from the vibrator being coupled into the slide. These transfer channels increase the cylinder volume, since, they must be filled and scavenged to the same pressure as the cylinder. The increased volume due to the channels is approximately 0.5 in.³.

This increased volume can be compensated for by a larger amplitude in slide motion. Allowance is made by lengthening the slide 0.375 in.

At this point it is appropriate to review the leakage rate which will occur with this design. The slide is 1/8 in. thick and 1 in. wide. The clearance surrounding the slide is approximately 0.005 in. giving a leakage area of 0.011 in.². This area is 20 percent of the calculated supply area and if leakage of the piston rings and seals is also included the total is about 25 percent of the supply area.

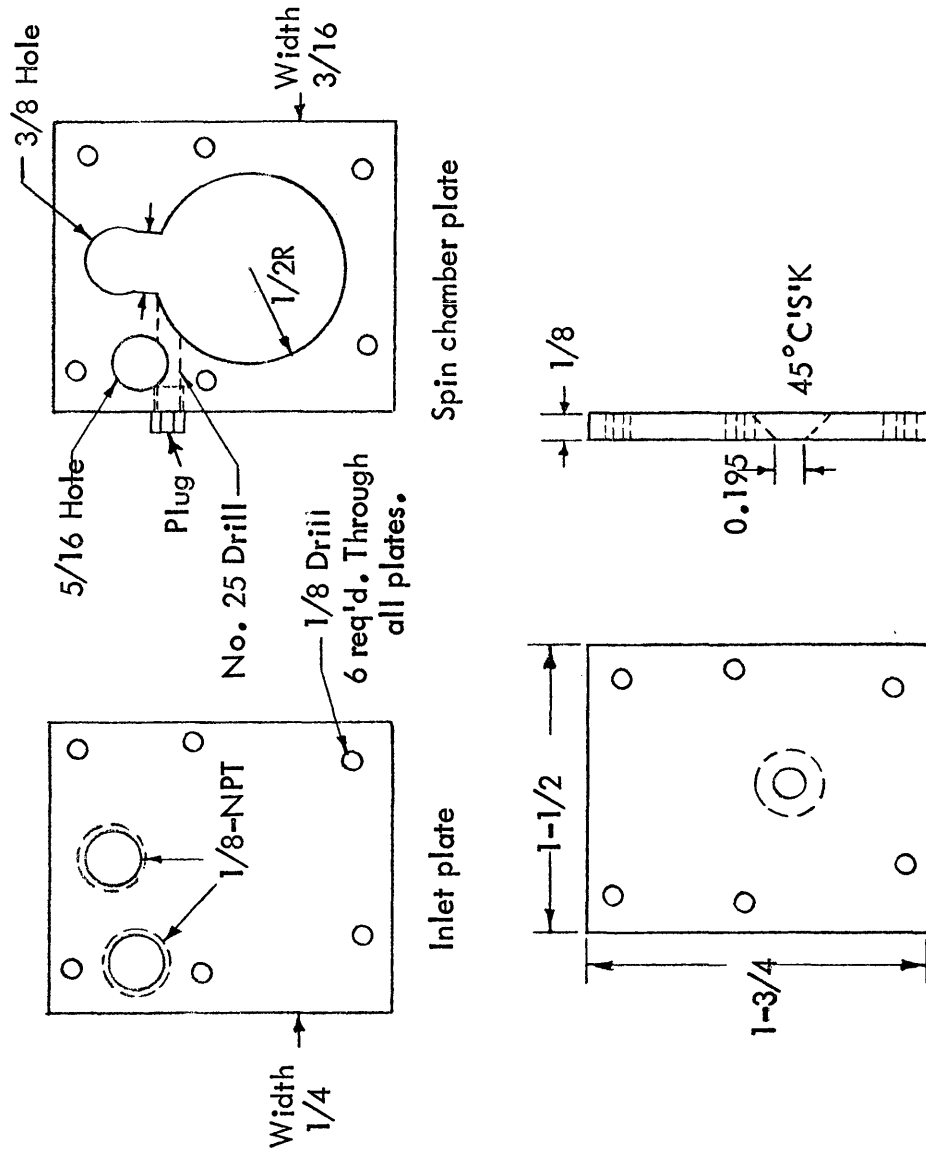
ANALYSIS OF FLUIDIC COMPONENTS

VORTEX AMPLIFIER

The derivation of required parameters for sizing the vortex amplifier must begin with a calculation of the pressure and flow required to drive the sliding plate. It is already known that the maximum pressure in the cylinder is 56 psia. This will be the maximum pressure that can be transmitted back via the feedback line to the control port of the vortex amplifier. Previous tests carried out with a test vortex valve operating on water indicate that for attainment of full vorticity the control pressure must exceed the supply pressure by approximately 20 percent. This implies that the vortex amplifier supply pressure should be about 40 psia. Assuming that under conditions of no control flow there is negligible pressure drop in the vortex valve except at the outlet orifice, the flow through the outlet can be calculated by using an upstream pressure of 40 psia and downstream pressure of 15 psia.

In the designed vortex valve the supply port area is twice that of the outlet port. This can be seen in Figure 10.

The slide system differs substantially from the piston-mass system in that the air which moves the slide must pass through the gap between vortex valve and flow pickoff. This feature is illustrated in Figure 12. Under these circumstances little of the vortex valve supply pressure can be regained when the outlet flow enters the slide cylinder through the flow pickoff.



Outlet plate
FIGURE 10. Detail of vortex amplifier.

The maximum attainable pressure in the slide cylinder is the stagnation pressure (Streeter, 1962, p. 389) of the outlet flow, and because of the gap the vortex valve outlet flow is not dependent upon the pressure in the slide cylinder.

An estimate of the required pressure to drive the slide can be calculated from the known weight of the slide, the amount of movement required and the frequency of operation.

Weight of slide	=	0.1875 pf.
Peak to peak amplitude	=	0.20 in.
Frequency	=	40 Hz.

The average velocity over a cycle is 16 in./sec. Assuming constant acceleration as before, the maximum velocity is 32 in./sec. and the acceleration needed is 5120 in./sec². This acceleration can be achieved by a force of 2.5 pf. Experiments were carried out to determine the steady state drag force on the sliding plate. This drag force is 2 pf. Therefore the vortex amplifier must have sufficient flow to develop 4.5 pf on the slide end plate. The diameter of the slide cylinder is 1.5 in. and the cross-sectional area is 1.765 in.². Hence, a pressure of 2.55 psi is required.

It is possible to estimate the flow velocity necessary to obtain a stagnation pressure of 2.55 psig. If the flow is isentropic then the velocity and pressure at a point upstream is related to the velocity and pressure at a point downstream by the following equation (Streeter, 1962, p.255).

$$\frac{U'_u{}^2}{2} + \frac{n}{n-1} \frac{P'_u}{\rho_u} = \frac{U'_d{}^2}{2} + \frac{n}{n-1} \frac{P'_d}{\rho_d}$$

Applying this equation to the gap between outlet orifice and flow pickoff the flow velocity at the pickoff is zero and the static pressure is approximately ambient at both points. This implies that the density remains relatively constant.

$$\rho_u = \rho_d$$

With these simplifications the velocity pressure relationship reduces to:

$$U'_u{}^2 = 2 \left(\frac{n}{(n-1) \rho_u} \right) (P'_d - P'_u)$$

At 14.7 psia and 150 °F the mass density of air is 1.17×10^{-6} slug/in.³.

Hence:

$$U'_u = \left[\frac{2(1.4)(2.55)}{(1.4-1)(1.17 \times 10^{-6})} \right]^{1/2} = 3900 \text{ in./sec}$$

Examination of Figure 11 shows that this spouting velocity is easily achievable with a pressure drop of only a few psi across the outlet orifice.

As previously mentioned the flow is not dependent upon the pressure in the slide cylinder, this allows the necessary flow to be determined by a simple filling rate calculation.

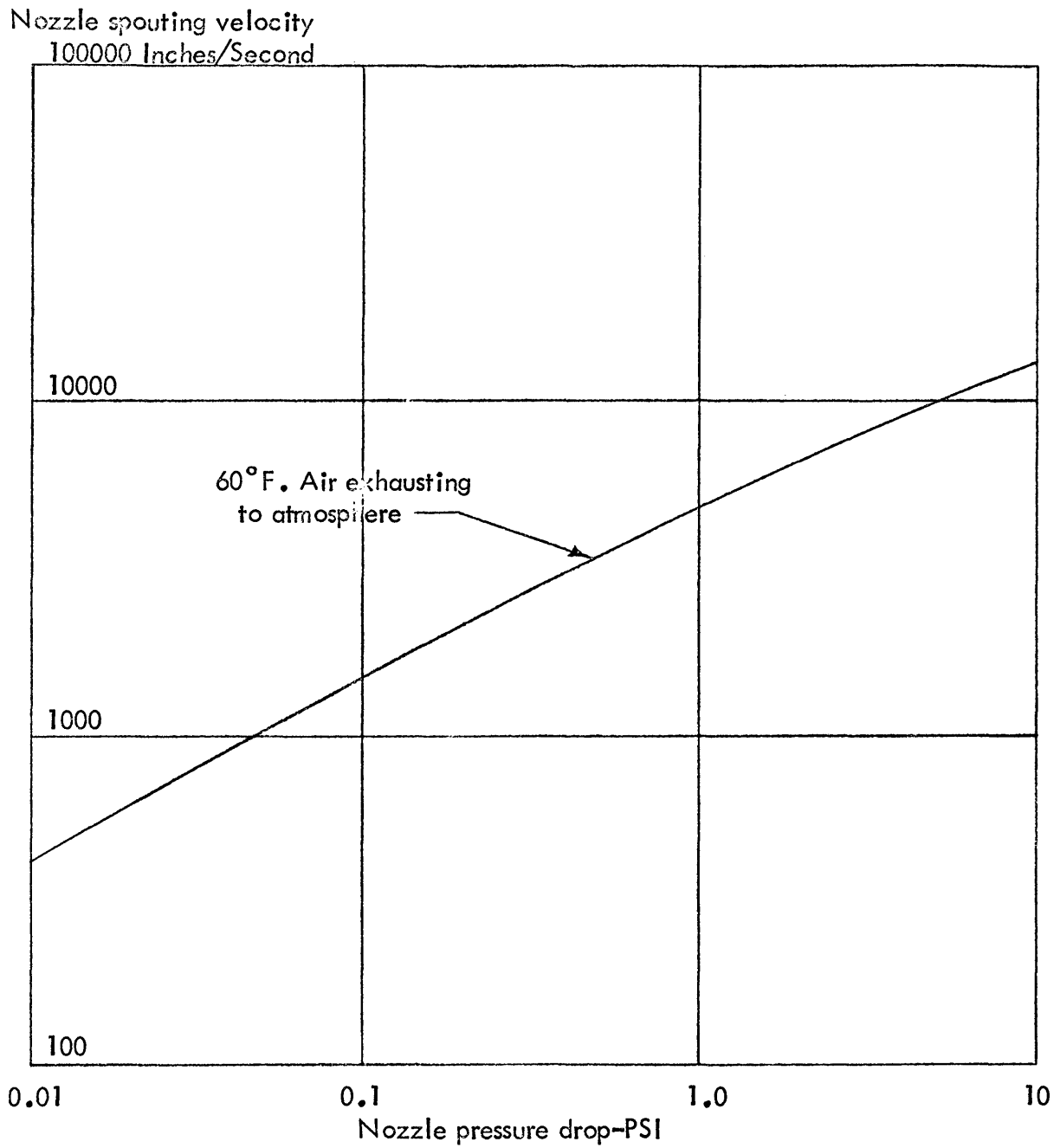


FIGURE 11. Spouting velocities for air.
(from Boothe, 1965, p.86)

Reference to Figure 12 shows the geometry and dimensions of the slide cylinder. Clearance was allowed in the cylinder for a total movement of $3/16$ in. in each direction. This additional movement was built into the plate valve to allow for the increased dead volume of the plate valve transfer channels. In actual fact an increase in amplitude from the design value of 0.065 in. to 0.1 in. proved to be adequate compensation. Hence, this value is used in the design of the vortex amplifier.

At the design frequency of 40 Hz it is anticipated that the switching time of the vortex amplifier from full vorticity to no vorticity will be only a small fraction of the period. The result of this will be that the vortex amplifier will drive the slide with an almost constant flow for one-half cycle and be shut off completely for the remaining half cycle. During half cycle of full vorticity the flow from the outlet orifice is in the shape of a cone. This swirl spray pattern is the result of the high vorticity in the spin chamber. This flow travels at high speed through the gap between the outlet orifice and the flow pickoff. This cone shaped jet, because of its high speed becomes completely turbulent almost instantly after leaving the outlet. Because of the turbulence the emerging jet entrains and mixes with the surrounding fluid. This entrained fluid is carried away by the jet leaving a low pressure region at the exit to the flow pickoff. This low pressure aids in scavenging the slide cylinder.

With a peak to peak amplitude of 0.2 in. there remains a space of 0.13 in. between the slide valve end plate and the end of the cylinder. This gives a dead

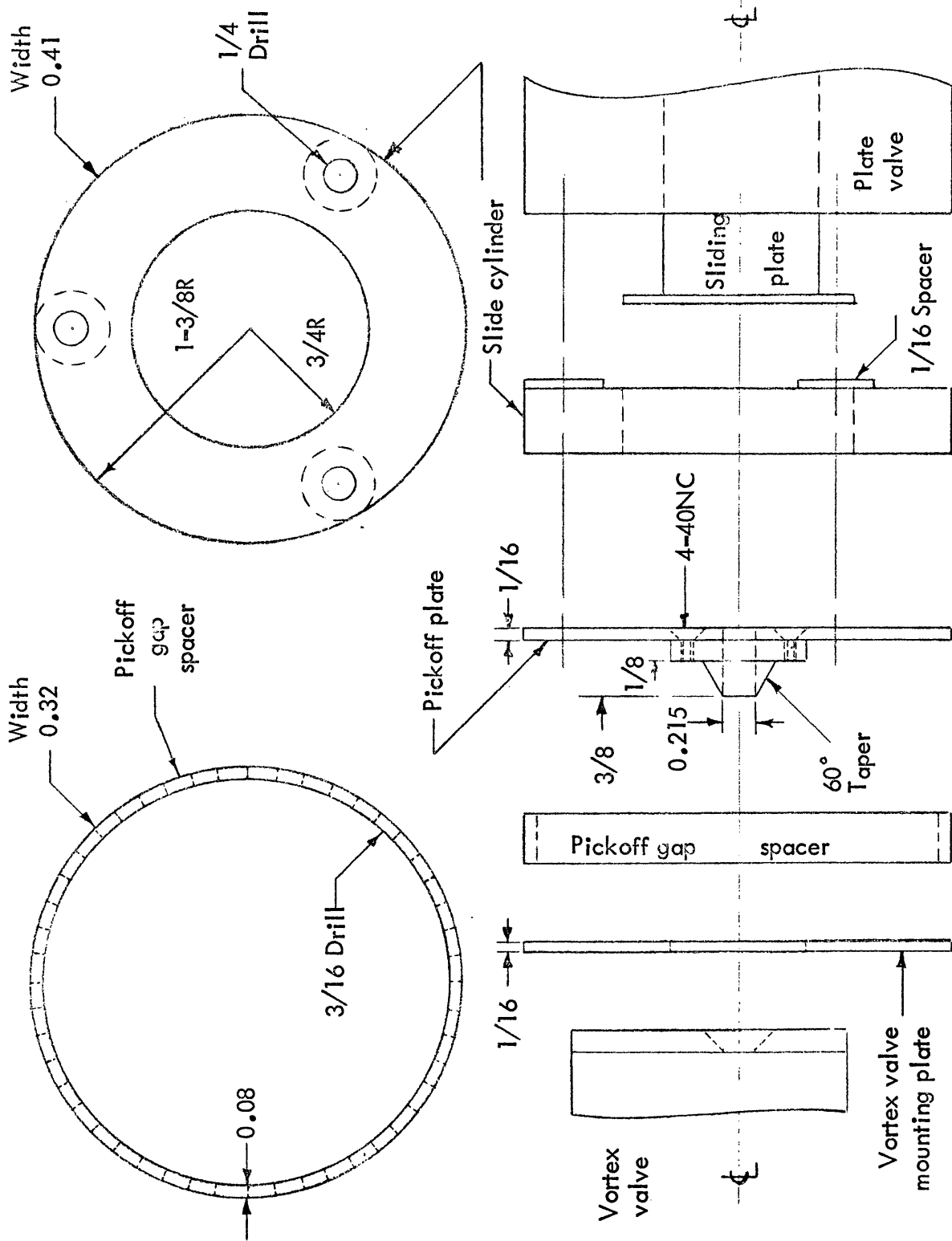


FIGURE 12. Detail of slide cylinder.

volume of 0.23 in.^3 . Assuming the cylinder is scavenged to ambient the dead volume will contain a mass of $3.24 \times 10^{-6} \text{ slug}$, calculated from the general gas law. Air is now admitted at a rate to move the slide 0.1 in. and to raise the pressure from ambient to 17.25 psia in $1/4$ cycle. The mass of air contained in the new volume at the high pressure is $6.72 \times 10^{-6} \text{ slug}$. The mass of air admitted during $1/4$ cycle = $6.25 \times 10^{-3} \text{ sec}$ is $3.48 \times 10^{-6} \text{ slug}$. This yields a filling rate of $5.57 \times 10^{-4} \text{ slug/sec}$.

It remains to determine the outlet orifice which will give this flow. For this purpose the orifice flow equation of Appendix A will be used.

$$A_{ud} = \frac{W_{ud} \sqrt{T'_u}}{K P'_u N_{ud}}$$

The upstream pressure in the vortex valve is 40 psia and the downstream pressure is ambient, this gives a value of $N_{ud} = 1.0$ from Appendix B .

$$A_{ud} = \frac{(0.0178)}{(0.532)} \frac{\sqrt{610}}{(40)} = 0.0207 \text{ in.}^2$$

The above value is the effective area, and the geometric area can only be calculated by considering the type of orifice being used. The orifice in the vortex valve is sharp-edged and beveled at 45° to allow for the swirl spray at high vorticity. The C coefficient for sharp-edged orifices is given in Appendix C . The coefficient depends upon the pressure ratio and upon the degree of bevel, with

steeper bevels having the highest coefficient. In this case the C coefficient has a value of approximately 0.84.

The geometric area becomes :

$$A = \frac{A_{ud}}{0.84} = 0.0246 \text{ in.}^2$$

Some allowance must be made for losses. The two most prominent losses are the leakage in the slide cylinder and entrance losses from the expanding jet as it enters the pickoff. An increase of 20 percent in the area is made to compensate. This determines the vortex valve outlet area of 0.0295 in.².

This size orifice was constructed and tried along with many other sizes but this original calculated value proved to be the best for operating the slide valve.

With the orifice area determined the next step is to determine the spin chamber diameter. Previous tests with a water vortex valve suggested that the ratio of outlet orifice diameter to spin chamber diameter should be approximately 1 to 5. The diameter corresponding to the orifice area is 0.195 in., consequently the spin chamber diameter is made 1.0 in.

Another important parameter for vortex valve operation is the curtain area. The curtain area is defined to be the ring shaped area in the spin chamber surrounding the outlet orifice. This area is calculated by multiplying the outlet orifice circumference by the spin chamber width. It is necessary that the curtain area be at least

twice the outlet area to prevent any flow restriction. The width of the spin chamber is $3/16$ in. hence the curtain area is 0.118 in^2 . This is 4 times the outlet area, which is more than adequate.

The spin chamber width was chosen in view of the requirement that the circular control orifice must be drilled through the spin chamber plate.

A larger curtain area than the one used can induce recirculating (formation of secondary vortices) flow in the spin chamber. This type of flow would be extremely detrimental to good vortex valve performance.

The sizing of the control orifice was done by experiment. Again the tests of the water vortex valve provided a useful guide. The rule of thumb obtained is to start with a control area equal to the outlet area and work down.

The proper control area depends upon the flow, via the feedback lines, that is exhausted from each side of the piston. This is controlled by blocking one of the double exhaust ports with a variable orifice. The best control area compromise obtained was 0.0177 in^2 . corresponding to a diameter of 0.15 in. This size gives stable operation of the vibrator over the entire frequency range from 40 Hz to 120 Hz.

The frequency may be regulated in two ways. The first is simply lengthening or shortening the feedback lines. For supply pressures above 120 psig the feedback line length and frequency relationship is given below :

4 in. (minimum length) 120 Hz

2.5 ft	70 Hz
5.0 ft	50 Hz
7.5 ft	30 Hz

The second method of changing frequency consists in varying the supply pressure to the vortex valve. This method is used to provide a sweep of frequencies and is described in the next section.

The only parameters not yet determined are the pickoff diameter and the gap between the outlet orifice and the pickoff.

The expansion of a jet from a circular orifice can be calculated but in this instance the existence of the pickoff in the jet disturbs the flow and makes it impossible to calculate. Hence, these two parameters were determined experimentally. The pickoff diameter was not as critical as the gap. The diameter chosen was quite naturally somewhat larger than the outlet orifice. The reason for the gap length being critical is that if too small it would force some flow into the slide cylinder during the entire cycle preventing proper scavenging. If the gap is too large, the effect of low pressure formation at the entrance to the pickoff would be diminished. The values for these two parameters are :

Pickoff diameter	0.215 in.
Pickoff tip to inside of spin chamber	0.203 in.

VIBRATOR SWEEP FREQUENCY AND
SELF STARTING MECHANISMS

The frequency of operation of the vibrator can be controlled by varying the supply pressure to the vortex amplifiers. The change in frequency can be due to two causes. One is the decrease in switching rate with the decrease in flow velocity through the spin chamber, the other is the decrease in flow into the slide cylinder resulting in a smaller peak to peak amplitude of the motion.

The criteria for the design of the sweep mechanism were the desire for reproducibility and for a simple method for making the system inoperative when it was not needed.

The sweep design can operate between any two frequencies within the range of the vibrator. The highest frequency is determined by the installed feedback line length. Sweeps always run from the highest to lowest frequency. As is shown in Figure 13 a push-rod operated valve is installed between the supply pressure adjusting valve and the supply flow dividing block. For constant frequency operation the push rod valve is left completely open. For a sweep the push rod valve is closed at an adjustable rate depending upon the frequency range desired and the length of the run. The closing rate is regulated by varying the air being admitted to an air cylinder operating the push rod valve. At the initiation of a run the vibrator timer actuates two magnetic valves. The main one is in the air line to the storage tank,

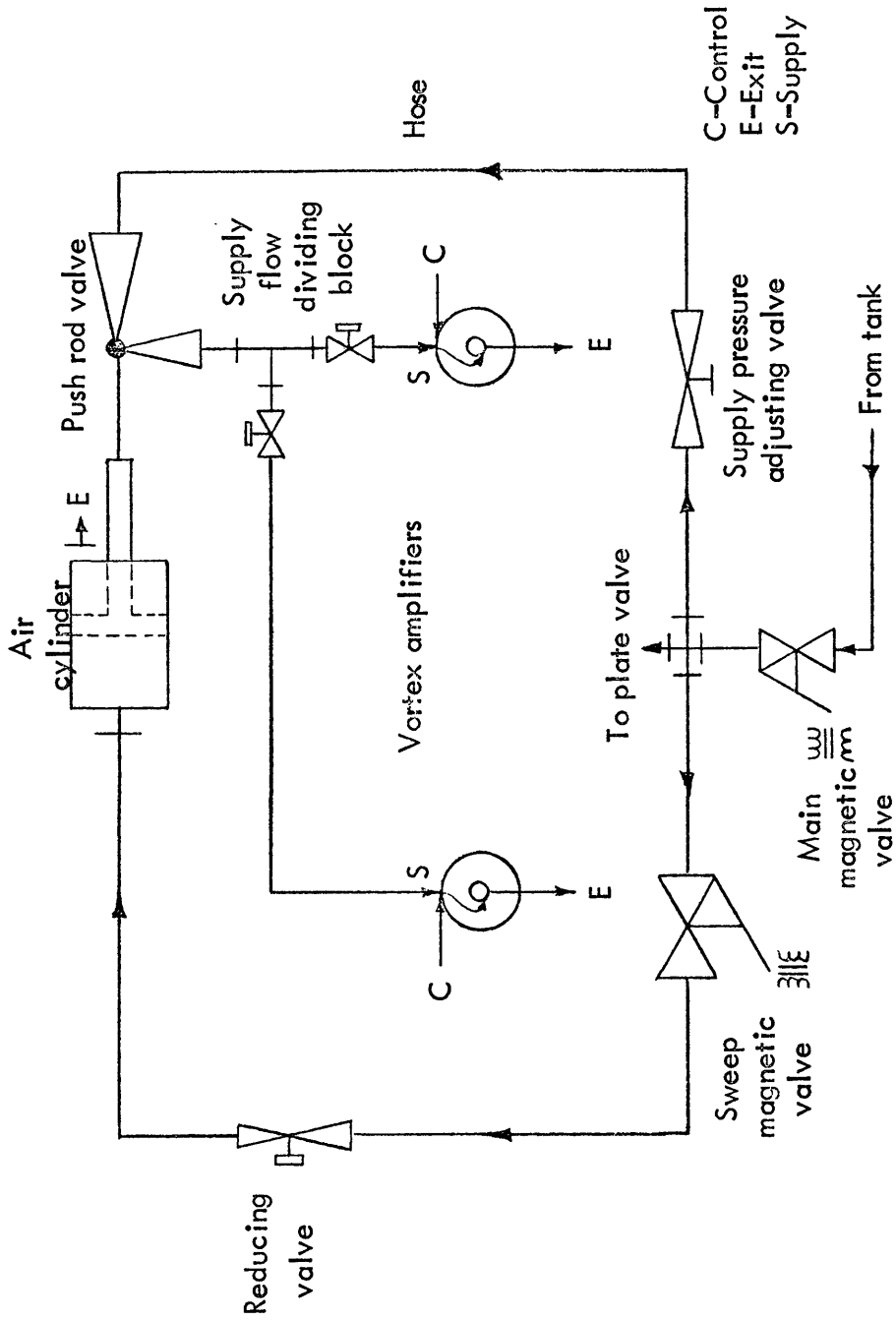


FIGURE 13. Sweep mechanism schematic.

the other taps air from between the main magnetic valve and the plate valve to operate the sweep mechanism.

This flow which is at tank pressure passes from the sweep magnetic valve into a variable metering orifice and then passes into the sweep air cylinder. The adjustment on the metering orifice is sufficient to control the push rod valve closing time interval from practically instantaneous to 15 seconds.

One additional adjustment can be made on the sweep mechanism. Between the air cylinder shaft and the valve push rod is a rod spacer. By shortening this spacer a delay can be made in the initiation of the sweep. Lengthening the spacer would decrease the frequency range of the sweep, because the run would start with the push rod valve in a partially closed position.

Upon actuating the main magnetic valve the air flows directly into the plate valve. Regardless of the location of the sliding plate, the vibrator will not be self starting since no pulse will be transmitted via the feedback line to the vortex amplifier. Consequently some provision must be made to make the vibrator self starting.

Self starting has been accomplished in this vibrator system by delaying the supply flow to one of the vortex amplifiers. The sequence of events takes place in the following order. A very light spring is placed between the slide end plate and the plate valve body so that the sliding plate will always be at one side when the run is commenced. Upon opening the main magnetic valve the air flows through the

supply pressure adjusting valve and the push-rod valve into the supply flow dividing block. The two outlets from this block go to the two vortex amplifier supply ports. Built into each outlet is a variable orifice which can be used to balance the vortex amplifiers. These adjustments are really trimmers to compensate for minor machining inaccuracies. Of primary importance is the length of each line from block to supply port. The short line goes to the same side as the slide. The longer line goes to the opposite side. The initial pulse from the opening magnetic valve reaches the slide side first and pushes the slide to the opposite side, this in turn charges one piston cylinder with air. At this time the delayed vortex amplifier starts and returns the slide back to its original position. This exhausts the piston cylinder which had just been charged and sends the first pulse down the feedback line thus initiating the continuous cycling.

VIBRATOR TIMER

Some means must be provided to time the length of run and to actuate the frequency sweep when this feature is needed. Initially, the recording truck supplies an electrical pulse to start the entire run sequence. The timer must provide outputs to the main magnetic valve and the sweep magnetic valve. These valves must then be kept open for the entire run period.

As shown in the schematic Figure 14, the timer uses two relays and one motor driven timer to accomplish the required functions.

Input to the vibrator timer can be any pulse with voltage in the range from 6 V to 12V. A current of 2.5 MA is required to trip the non-locking relay. An input potentiometer and panel mounted milliammeter are provided to adjust the incoming pulse to give this current. Closing the non-locking relay in turn closes the latching relay. This latching relay is activated by 26.5 VDC supplied from a 45V battery. The 26.5V is tapped from an adjustable potentiometer which is connected across the battery terminals. A D.C. voltmeter is provided on the front panel to monitor the setting of the potentiometer to 26.5 VDC. Further adjustment of this potentiometer would be necessary only if the battery output drops below 45V. The latching relay is controlled by a three way switch. The positions of this switch correspond to latch, off and unlatch. In preparation for a timed run the relay must first be unlatched. This is accomplished by placing the three position switch in the

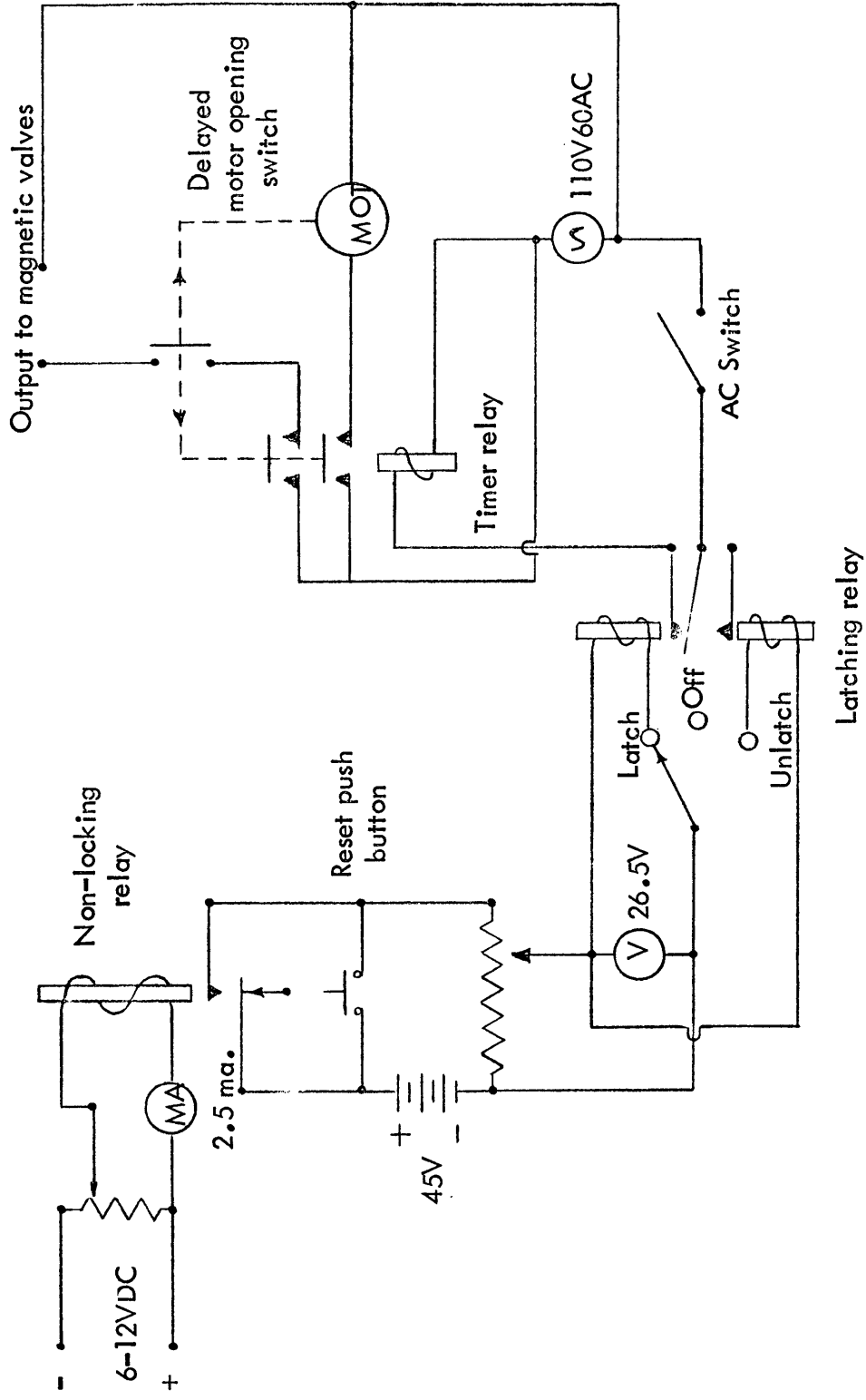


FIGURE 14. Schematic of timer.

unlatch position and opening the relay with a pulse from the reset push button. This reset is placed in parallel with the non-locking relay and obviates the supplying of a pulse from the recording truck to reset the timer or initiate a timed run. After resetting the latching relay the three position switch must be returned to its latch position. The timer can then be made ready to operate by placing the 110 V A C switch in the on position.

A pulse from the recording truck or from the reset push button will now close the latching relay. This relay provides 110 V A C to actuate the timer solenoid which starts the synchronous timer motor. This solenoid closes two timer switches which provide the 110 V A C output to the main magnetic valve and the sweep magnetic valve. After the preset time has elapsed the timer opens the two switches and the run ends. The operator at this point should return the 110 V A C switch to the off position in order to shut off power to the timer solenoid. Normal field procedure is to reset timer for the next run as described in the previous paragraph.

One caution should be noted in the operation of the vibrator timer. This is that the three position switch should not be left in the off position. Any pulse from the recording truck or reset push button will place excessive voltage across the terminals of the latching relay voltmeter. The reason for this is that the latching relay resistance is no longer in parallel with the voltmeter.

Note : The scale markings on the Microflex timer are not correct. The original timer motor has been replaced by a higher speed motor. One division on the scale now corresponds to 0.25 second.

ACCESSORY EQUIPMENT

The operation of the timer and magnetic valves requires a 110 V A C electrical source. The maximum power consumption of the system is 70 watts. Therefore any small DC to AC converter will be adequate. The output waveform should be sinusoidal. Of greatest importance is the requirement that the frequency be stable. Any change in frequency from 60 Hz will affect the speed of the synchronous timer motor and subsequently give erratic variations in the length of run. This problem has been encountered in field tests.

An accurate pressure gauge must be provided on the storage tank. This is to insure that each run begins at the same starting pressure.

For the field tests an inline water separator and lubricator were used. The main purpose was to prevent any corrosion on the interior steel parts due to water droplets. The field tests were run for four days and no corrosion was noted at the end of this period. The lubricator was used to inject small amounts of kerosene into the supply air to displace any water not eliminated by the separator.

The plate valve does not require lubrication, since the sliding plate is cushioned by air on all sides. A small amount of kerosene does assist in preventing any sticking of the rubber piston rings and cylinder end seals.

A Kistler dynamic pressure gauge is installed in the driving cylinder to provide a monitor of the pressure fluctuations. The output of the pressure gauge is adequate to be used as the input to an oscilloscope, strip recorder or recording truck system. This output can be used to adjust the vibrator frequency or sweep. In addition, it can provide a time break for refraction studies and a reference signal for correlation.

FIELD TESTS OF VIBRATOR

The field tests were conducted with two goals in mind. The first of these was to determine if the energy output of the vibrator was sufficient to make the unit practical for near-surface work. It was also desired to determine if the unit was reliable and if any weakness existed in its design. It has been noted previously in this report that during the four days of operation the unit performed reliably with no difficulties encountered.

Before discussing the field tests in detail it will be useful to review the main characteristics of the vibrator unit.

The total weight of the unit is approximately 150 pf. It can be operated horizontally or vertically and, since the mass and spring housings are sealed, it can be partially buried to assist in making a good ground contact.

The power of the vibrator at 40 Hz is 2.9 hp (Crane Industrial Products Group, 1957, p.B-8) and the maximum kinetic energy of the piston-mass system has a value of 54 ft-pf. The amount of energy actually transferred to the ground is not known because of the difficulty in estimating the ground coupling. The power and energy of the vibrator indicate that it is more than twenty times as powerful as the electromagnetic system used by Howell (1940,p.1) whereas it has only 1/200 the energy of a "Vibroseis" system.

All tests were conducted using a 200 psig compressor system. With this pressure the total air consumption rate was 154 SCFM. The vibrator

can be run at any fixed frequency between 30 and 120 Hz, including single pulses. The sweep mechanism can be set to give a sweep over any part of the frequency range, always starting at the high frequency and ending at the low frequency.

The tests were made at three different locations near Denver, Colorado. These are the Biddle Farm near Mead, the Ken-Caryl Unit of the McDannald Ranch south of Denver, and South Table Mountain in Golden. The first two areas are situated on Pierre Shale. The Golden area is a lava flow with only a few feet of loose soil on top. At the Biddle Farm the bedding of the shale is almost horizontal, whereas at the McDannald Ranch the dip is approximately seventy five degrees toward the east.

It was necessary to develop an operational recording technique which differs somewhat from the normal explosive recording sequence. The vibrator can be run repeatedly to adjust the recording amplifiers. Therefore the normal automatic gain control system was dispensed with. The amplifiers were tapered, that is, the output of the geophones nearest the source were attenuated to a greater extent than the ones further away. A geophone separation distance of ten feet was chosen to give a good alignment of adjacent traces. One 14 Hz geophone was placed at each of the twenty four recorder inputs. The first geophone in all cases was located ten feet from the vibrator and this placed the last geophone in the line two hundred forty feet from the source. The vibrator was partially buried at all locations. Efficiency of coupling to the ground was dependent upon location and the Table Mountain area presented the poorest coupling. It was clear from the tests that the

earth material acts as a selective filter by transmitting certain frequencies and rejecting others. On some of the records there is a large pulse at the beginning and end of each run. This is due to the piston-mass hitting the lower stop in the vibrator. Although there was very poor coupling at the Table Mountain site no difficulty was encountered in transmitting 50 Hz energy from these pulses to the last geophone.

With the basic recording procedure decided upon, field data was collected to investigate certain features of the vibrator system. These are in order of their presentation in this report, (1) an investigation of the effect of increased weight and packing around the vibrator, (2) a repeatability test to determine the possibilities of stacking seismic energy to reduce random noise levels on the record, (3) a check out of vibrator operation over a range of frequencies with different recording filter adjustments, and (4) examination of the vibrator records to determine what types of waves have been generated.

The coupling characteristics tests are shown in Figure 15. The figure is made from tracings of the record monitors. Trace A was made with the vibrator operating normally. Trace B is a repeat of A with the addition of a mans weight on the vibrator, about 150 pf. Trace C repeats trace A again except the vibrator was packed in the ground with a heavy mud. The tracings indicate some variation in coupling.

The greatest increase in coupling is most noticeable at the

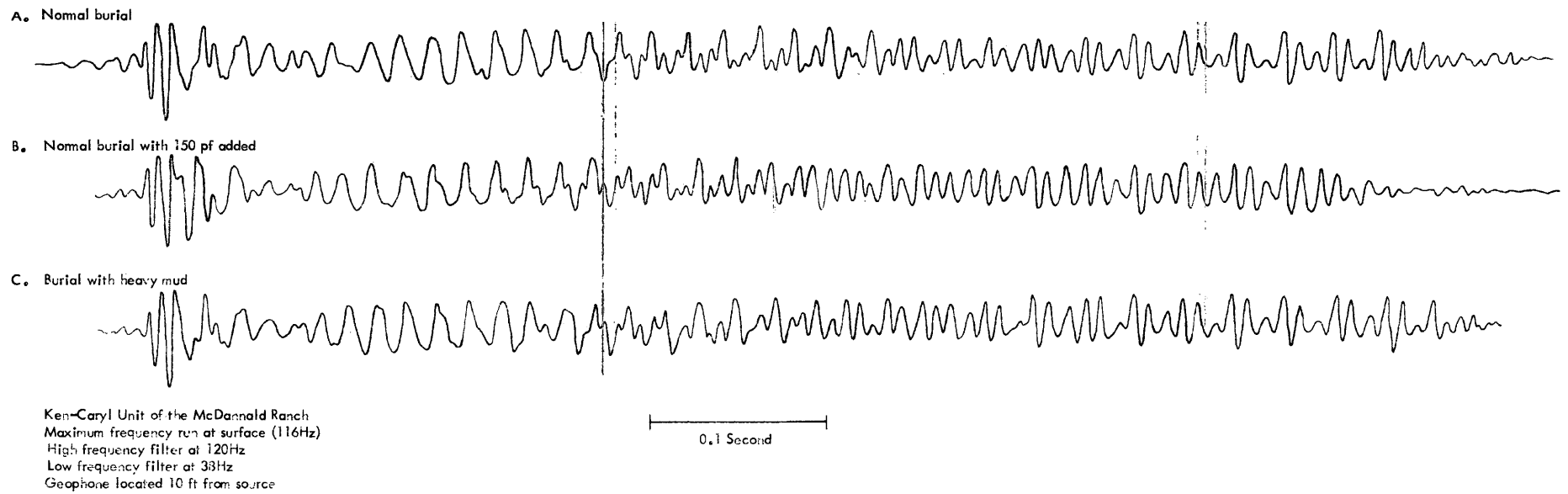
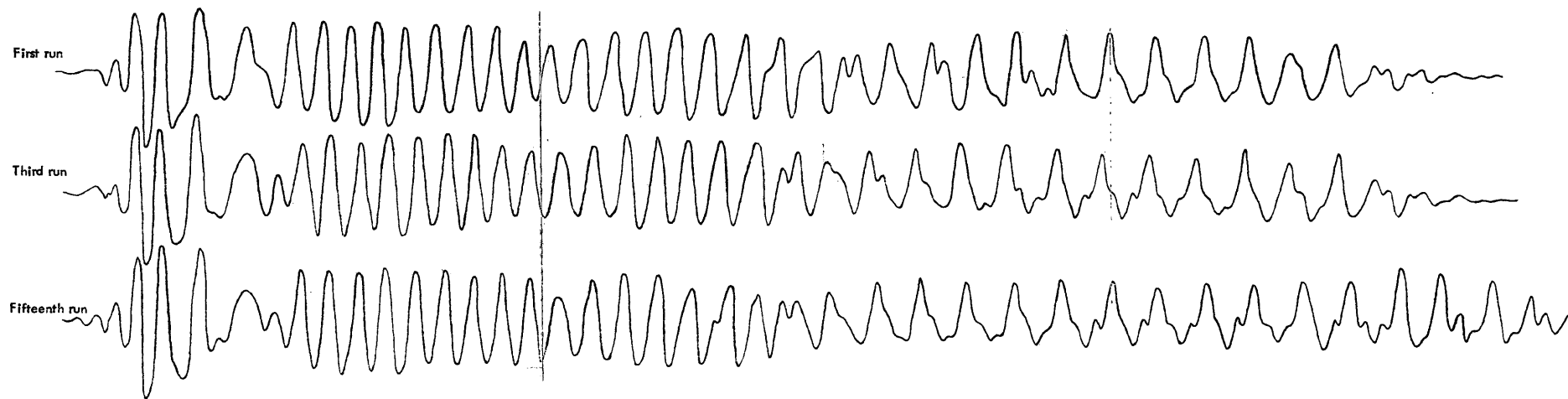


FIGURE 15. Ground coupling tests.

highest frequency and with the additional weight. Run B is slightly shorter than the other two. This can be attributed to a more rapid damping of the oscillation with the increased weight. It is worth noticing the reproducibility of the vibrator in these three consecutive runs.

Additional reproducibility tests were made at the Biddle Farm using a frequency sweep of 90 to 30 Hz. A total of twenty three runs were made of which the first, third and fifteenth are shown in Figure 16. Some phase shifting has occurred between the first and third runs. This phase shift may be the result of the vibrator settling in its partially buried location. The third and fifteenth runs are almost identical except that the fifteenth run is slightly longer. This lengthening of run is due to the frequency output of the DC to AC converter decreasing under additional load causing the timer motor to run slower. These tests indicate that the vibrator should be run several times to allow for settling before record stacking is attempted. Also, the AC source should be used to drive the vibrator electrical equipment only, so that, the electrical load remains the same for each run.

A representative record from the McDannald Ranch is given in Figure 17. In this figure the predominant alignments can be seen. This figure may also be roughly compared with the records obtained by Dobrin and others (1951, p.825) from small surface explosions. The vibrator run is of course longer than the explosion but by looking at the first part of the vibrator record many similarities can be seen. The high speed body wave phases appear on the first



Biddle Farm
Sweep input 90Hz to 30Hz
High frequency filter at 120Hz
Low frequency filter at 27Hz
Geophone located 10ft from source

FIGURE 16. Reproducibility tests.

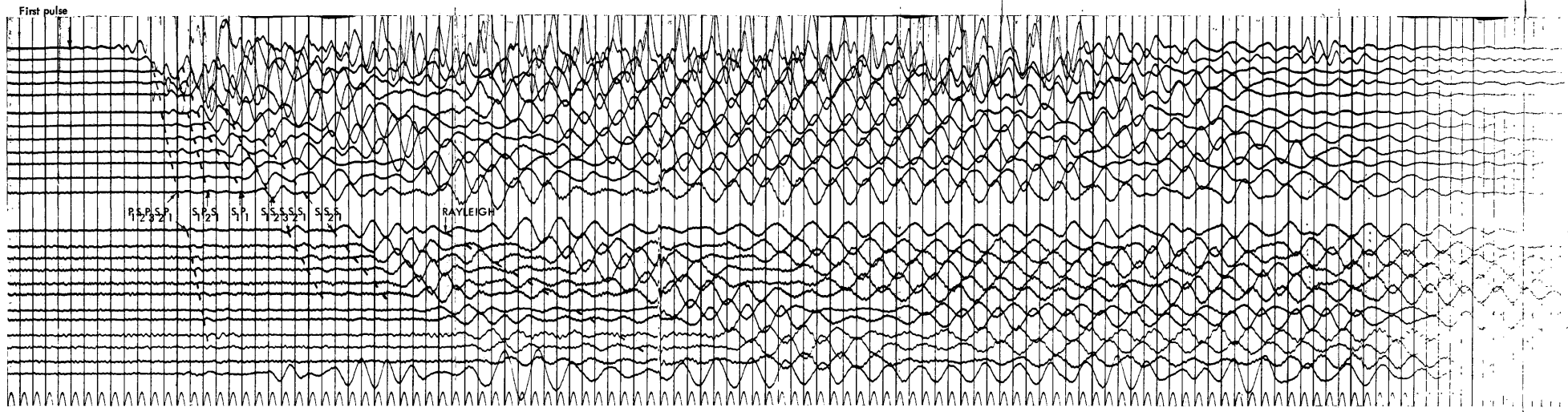


FIGURE 17. Field record from the Ken-Caryl Unit of the McDannald Ranch.
 Run at 50 Hz. Tape No. 353498
 High frequency filter at 90 Hz
 Low frequency filter at 38 Hz
 Each division on record is 10ms
 The first geophone is located 10ft from vibrator.
 Geophone spacing 10ft
 The last trace is trace 13
 Duration of run 1 second

EVENT	CRITICAL DISTANCE	VELOCITY
S ₁ S ₂ S ₁ (S ₂)	34ft	1170 ft/sec
S ₁ P ₁ (P ₁)		1800 ft/sec
P ₁ S ₂ S ₁ P ₁ (S ₂)	41ft	2100 ft/sec
S ₁ P ₁ S ₁ (P ₁)	9ft	3670 ft/sec
P ₁ S ₁ P ₁ S ₁ (P ₁)	31ft	4870 ft/sec
Rayleigh		570 ft/sec

part of the record. The point on the vibrator record where Rayleigh energy begins to dominate can be plainly seen as it can also be seen on the explosion record. A significant difference between the records is that there is little, if any, observable dispersion of the Rayleigh waves on the Pierre Shale vibrator records.

Figure 18 is a plot of the various wave speeds obtained from the records made at the McDannald Ranch.

Figure 19 shows the occurrence of the first pulse associated with each velocity and the range over which it appears on the records. However, when using Figure 19 one should keep in mind the emergent nature of the Rayleigh wave.

An estimate of the depth to the sub-weathering layer can be obtained from other experiments carried out on the Pierre Shale in eastern Colorado. The depth from these experiments ranges between 27 and 50 ft.

The slowest wave speed (570 ft/sec) was identified as the Rayleigh wave. This event is the slowest and strongest observed on the record. Theoretical curves of Rayleigh wave dispersion can be found in Ewing and others (1957, p.205). These curves are normally plotted with the ratio of Rayleigh velocity to upper layer shear speed on the ordinate and the dimensionless horizontal wavelength $2\pi/kH$, on the abscissa (Here k is the wave number of the Rayleigh wave and H is the thickness of the upper layer). If H is assumed to be 28 ft then the values of $2\pi/kH$ obtained during the field tests at the McDannald Ranch are as plotted on Figure 18. For the Rayleigh waves

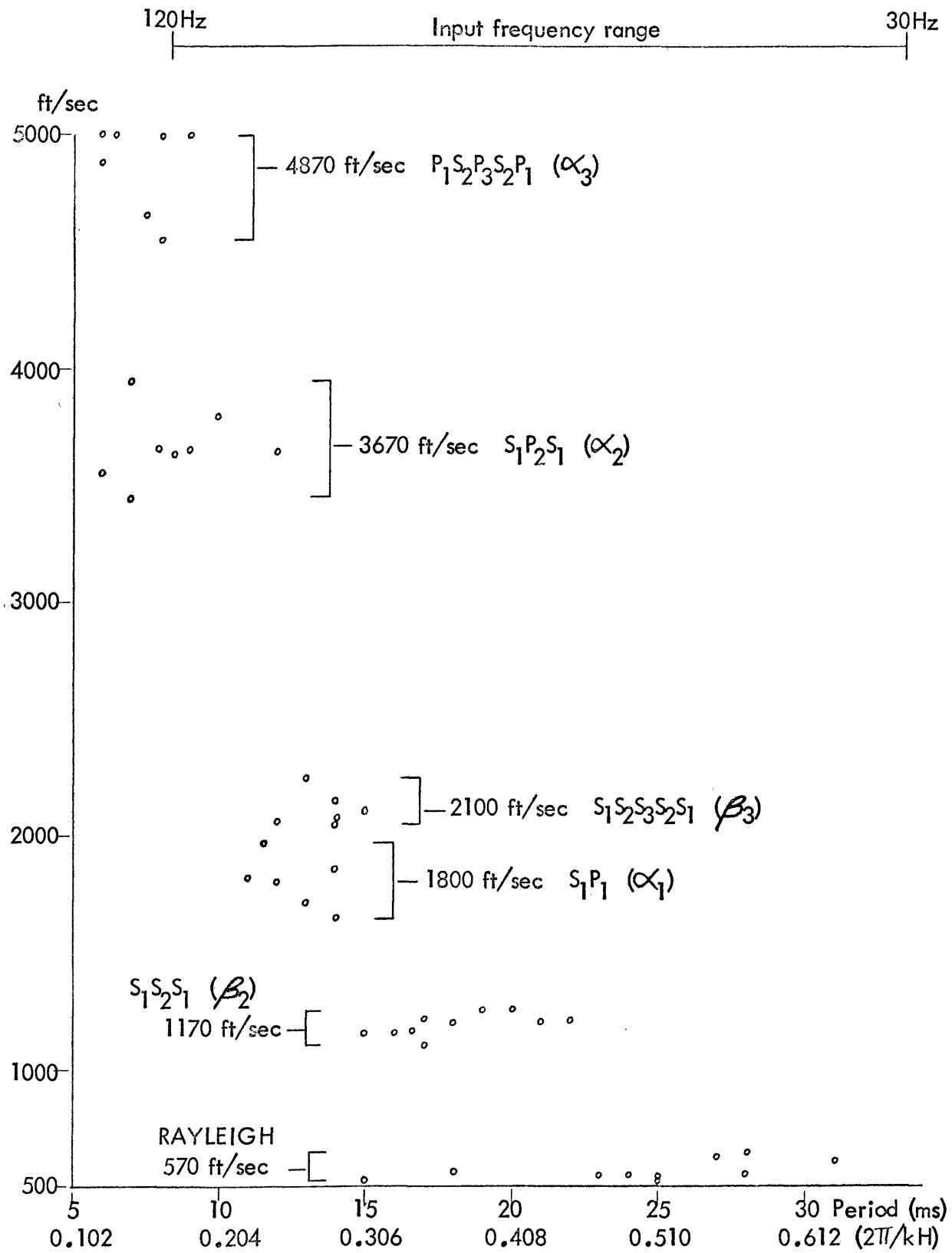


FIGURE 18. Average velocities Ken-Caryl Unit of the McDannald Ranch. (H=28ft)

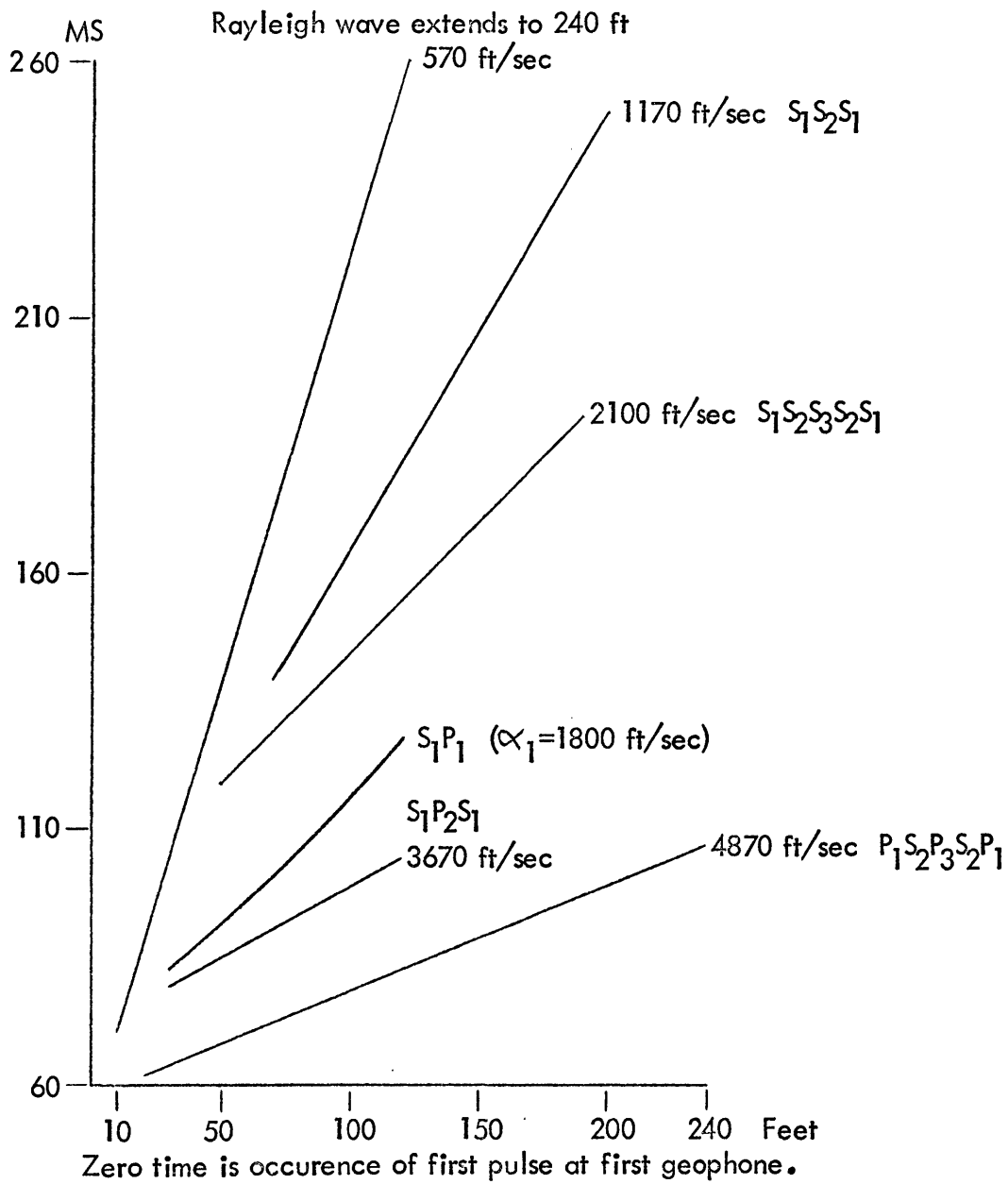


FIGURE 19. Time-distance plot for surface and body waves at the Ken-Caryl Unit of the McDannald Ranch.

observed at the McDannald Ranch the range of values extends from 0.306 to 0.632. When this parameter becomes this small it implies that the relationship between upper layer shear speed β_1 and Rayleigh phase velocity c is the same as that which is found in the homogeneous half space analysis.

Examination of the curves given in Ewing reveals further that for small values of $2\pi/kH$, c is approximately equal to the Rayleigh wave group velocity U . This rules out any possibility that the observed Rayleigh wave is generated by sound from the vibrator. To have air coupling the speed c must be approximately the same as the speed of the air wave and this condition is not met.

For earth materials with a Poisson's ratio of 0.25 the relationship between U and β_1 is $U = 0.92 \beta_1$. Using measured value of U and calculating $\beta_1 = U / 0.92$, the Rayleigh phase velocity equation can be checked for consistency. The velocity of α_1 can be obtained from the reflection S_1P_1 and the calculated value of β_1 . If the result of the Rayleigh equation calculation is not zero then a new ratio between β_1 and U can be postulated and the process repeated. By this iteration the ratio was found to be 0.93. Hence, β_1 can be calculated to be 610 ft/sec and $\alpha_1 = 1800$ ft/sec. Poisson's ratio for $\alpha_1 = 1800$ ft/sec and $\beta_1 = 610$ ft/sec is 0.436. The remaining velocities are interpreted in terms of body waves.

As can be seen from the grouping about 2000 ft/sec in Figure 18

the separation of these measurements into two distinct waves is not accurate.

The 2100 ft/sec speed is interpreted as being β_3 , the shear speed of the lowest observed layer. The scatter of the points representing this event in Figure 18 is attributed to interference with the S_1P_1 reflection.

Poisson's ratio for $\beta_2 = 1170$ ft/sec and $\alpha_2 = 3670$ ft/sec is 0.444.

For the deepest layer, $\beta_3 = 2100$ ft/sec and $\alpha_3 = 4870$ ft/sec. These values yield a Poisson's ratio equal to 0.386. These values are reasonable for the near-surface layer and they agree with the data from the Biddle Farm which is also located on Pierre Shale.

It might be postulated that the 1170 ft/sec velocity is the result of an air wave rather than a compressional wave. On the day the tests were made the air temperature was approximately 80 °F. The speed of sound at this temperature is 1140 ft/sec. The small difference in velocity of 30 ft/sec cannot be positively distinguished from the records. The speed of sound varies directly as the square root of the absolute temperature and the records were examined to see if variations existed between midday and late evening. No variation was detected, however, the expected variation is only about 30 ft/sec and this is too small to be detected with certainty. The strongest evidence to discount the possibility of an air wave is the fact that no wave speed in the neighborhood of the speed of sound was detected at the other locations. The sound waves emitted by the vibrator differ from a surface explosion in that they are of a known frequency. This fixed frequency air wave should act as a forcing input to the ground. However, no correspondence

was found in the records between the frequency of the air wave and the frequency of the 1170 ft/sec wave. The range of frequencies from the vibrator extend between 120 and 30 Hz. The frequency range of the 1170 ft/sec wave was only 65 to 40 Hz.

McDonal and others (1958, p.424) have reported measured velocities in Pierre Shale at a depth of 500 ft.

Compressional velocity	7380 ft/sec
Shear velocity	2680 ft/sec

These values give a Poisson's ratio of 0.42. This suggests the value obtained from the data for the lowest observed layer may be somewhat small.

A closer comparison can now be made with published dispersion curves by using the calculated values from the McDannald Ranch.

$$\frac{\alpha_2}{\beta_1} = 6.02 \quad \frac{\alpha_1}{\beta_1} = 2.95 \quad \frac{\beta_2}{\beta_1} = 1.92 \quad \frac{\mu_2}{\mu_1} = 3.68$$

where μ is Lamé's constant.

Since no significant change in density is expected between the layers, $\rho_2 = \rho_1$.

These values are roughly equivalent to those used in case 6, of Ewing and others (1957, p.206). For $2\pi/kH$ less than 0.65 the Rayleigh group and phase velocities are approximately equal and $U = 0.93\beta$ is in agreement with the assumptions made.

Some further information can be gained from examination of the locations at which the events occur on Figure 19. The time of occurrence of

the wave, from the first pulse observed at the first geophone is given. It is assumed that the first pulse left the vibrator 10 ms previously.

An estimate of the thickness of the refracting layers can be made from the intercept times, T_i (Knox, 1967, p.200). For the β_2 refraction this is 88ms and for α_2 it is 82 ms. The β_2 and α_2 refractions are thought to be made up of $S_1S_2S_1$ and $S_1P_2S_1$ travel paths. The thickness of the first layer can be calculated from

$$H_1 = \frac{T_i}{2(1/V_1^2 - 1/V_2^2)^{1/2}}$$

For $S_1S_2S_1$, the replacement $V_1 = \beta_1$ and $V_2 = \beta_2$ yields 31.4 ft and for $S_1P_2S_1$, 25.3 ft. This gives an average depth of 28 ft for the first refractor.

A similar procedure can be carried out for the second layer.

$$H_2 = \frac{T_i - 2H_1(1/V_1^2 - 1/V_3^2)^{1/2}}{2(1/V_2^2 - 1/V_3^2)^{1/2}}$$

The intercept times for β_3 and α_3 are, respectively, 105 ms and 68 ms.

Assuming transmission paths of $S_1S_2S_3S_2S_1$ and $P_1S_2P_3S_2P_1$ yields 12 ft and 23.4 ft for the thickness of the second layer. This difference in depth may be due to inaccuracies in velocity and time measurement. Taking the average depths $H_1 = 28$ ft and $H_2 = 18$ ft, the critical refraction distances, which are distances to the point at the surface where the refraction should first appear, can be calculated they are:

$$S_1S_2S_1 = 34 \text{ ft}$$

$$S_1P_2S_1 = 9 \text{ ft}$$

$$S_1 S_2 S_3 S_2 S_1 = 41 \text{ ft}$$

$$P_1 S_2 P_3 S_2 P_1 = 31 \text{ ft}$$

With respect to the surface wave its intercept time indicates that it is not from the first pulse generated by the vibrator. For a Rayleigh wave this may not be unreasonable since the Rayleigh wave transmission factor is of infinite length while those of the far field body waves are impulsive (Cagniard, 1962, p.179).

An example of the records obtained at the Biddle Farm is shown in Figure 20. The data from this area is simpler than that from the McDannald Ranch. In Figure 21 only three velocity groupings are found. The average speeds calculated from these groupings are given in Figure 21.

The thickness of the upper layer is assumed to be 28 ft as before, therefore the parameter $2\pi/kH$ has approximately the same values as before and the same reasoning applies. The upper layer shear wave $\beta_1 = 550 \text{ ft/sec}$ is calculated from $U = 0.93 \beta_1$. The 2860 ft/sec wave of Figure 22 was interpreted as the lower layer shear wave refraction $P_1 S_2 P_1$. The critical distance for this refraction is 34 ft and the thickness of the upper layer can be calculated as before to be 29 ft. No higher velocity refraction was found to correspond with this event. Interpretation of the second coherent event on the records as $P_1 P_1$ yields a near-surface compressional speed of 1440 ft/sec. Poisson's ratio for the surface layer becomes 0.416. This value compares favorably both with the data from the McDannald Ranch and the values obtained by McDonal, et. al. The measured shear speed of 2860 ft/sec is 180 ft/sec higher than found by McDonal.

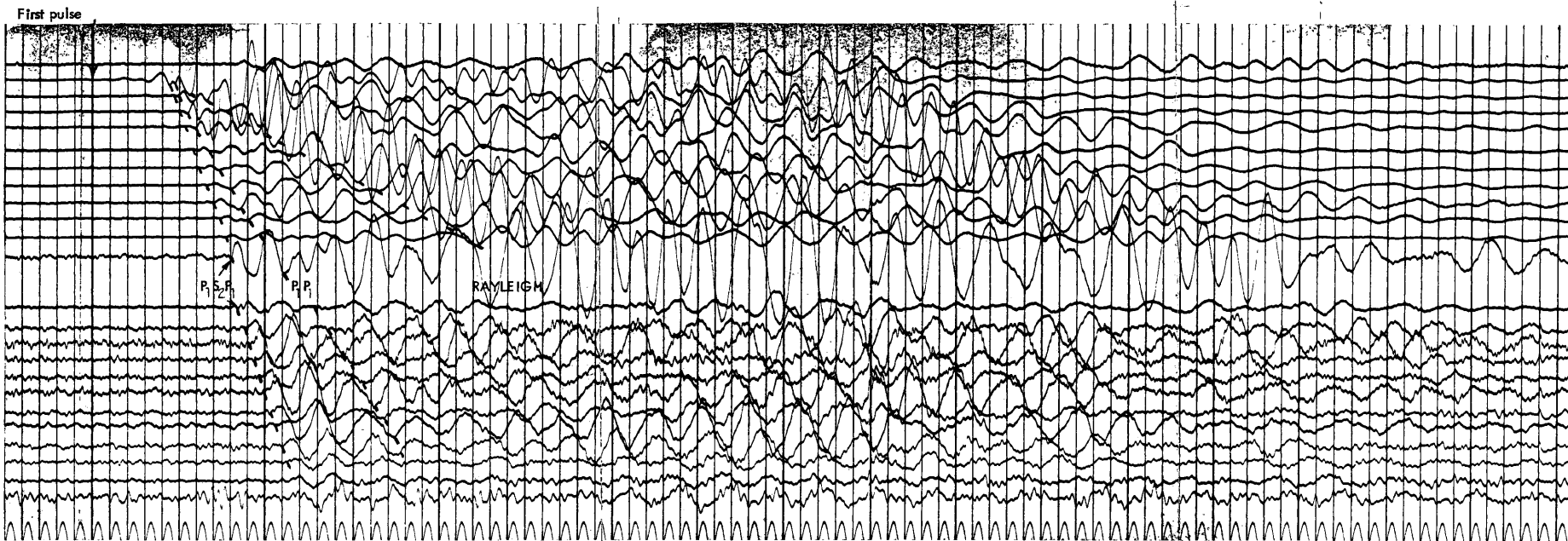


FIGURE 20. Field record from the Biddle Farm.
 Run at 30Hz. Tape No. 353648
 High frequency filter at 47Hz
 Low frequency filter at 20Hz
 The first geophone is located 10 ft from the vibrator.
 Geophone spacing 10 ft
 Each division is 10 ms
 The first trace is trace 12
 Duration of run 510 ms

EVENT	CRITICAL DISTANCE	VELOCITY
$P_1 S_2 P_1 (\beta_2)$	34 ft	2860 ft/sec
$P_1 P_1 (\alpha_1)$		1440 ft/sec
RAYLEIGH		510 ft/sec

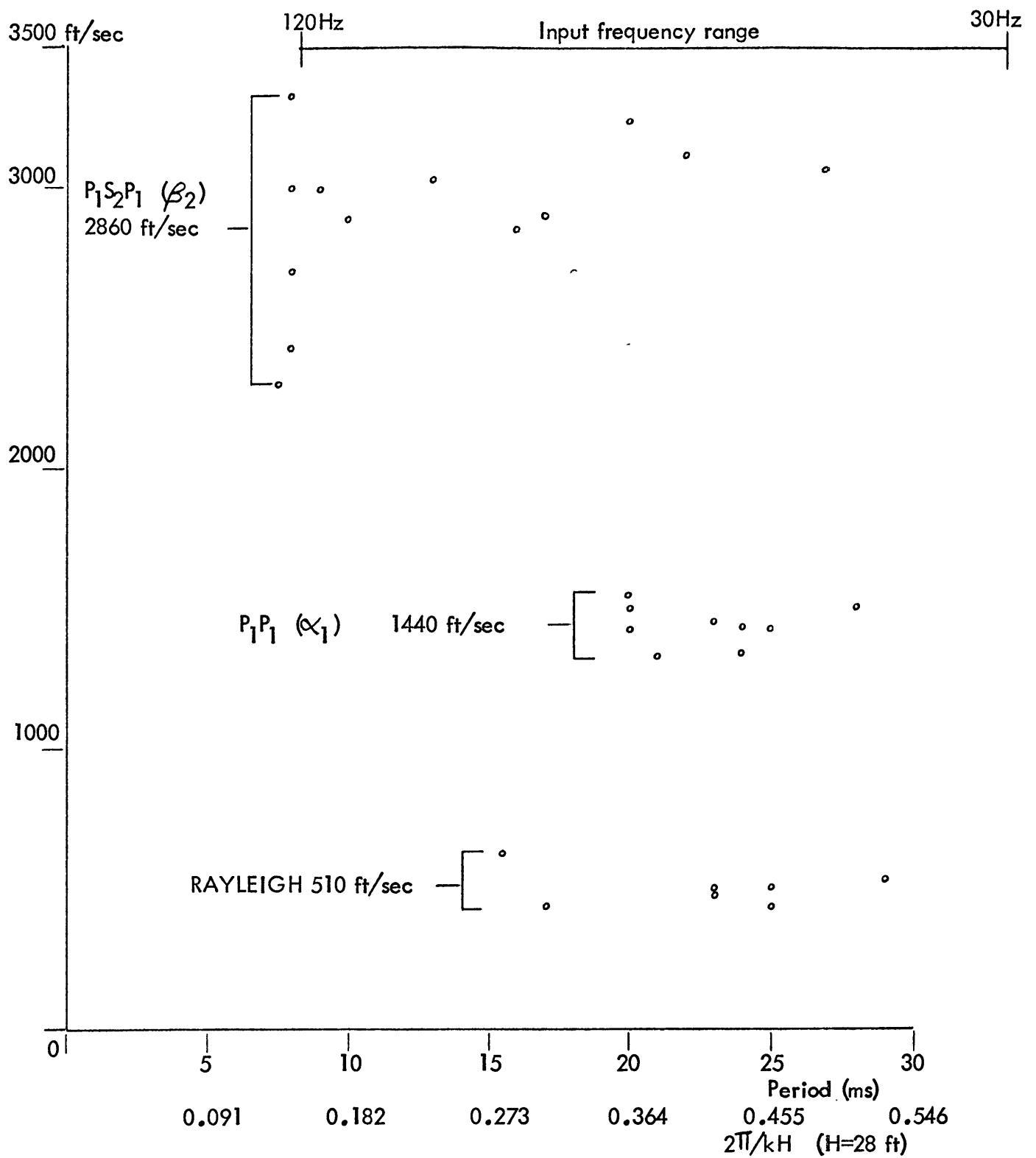


FIGURE 21. Average velocities Biddle Farm.

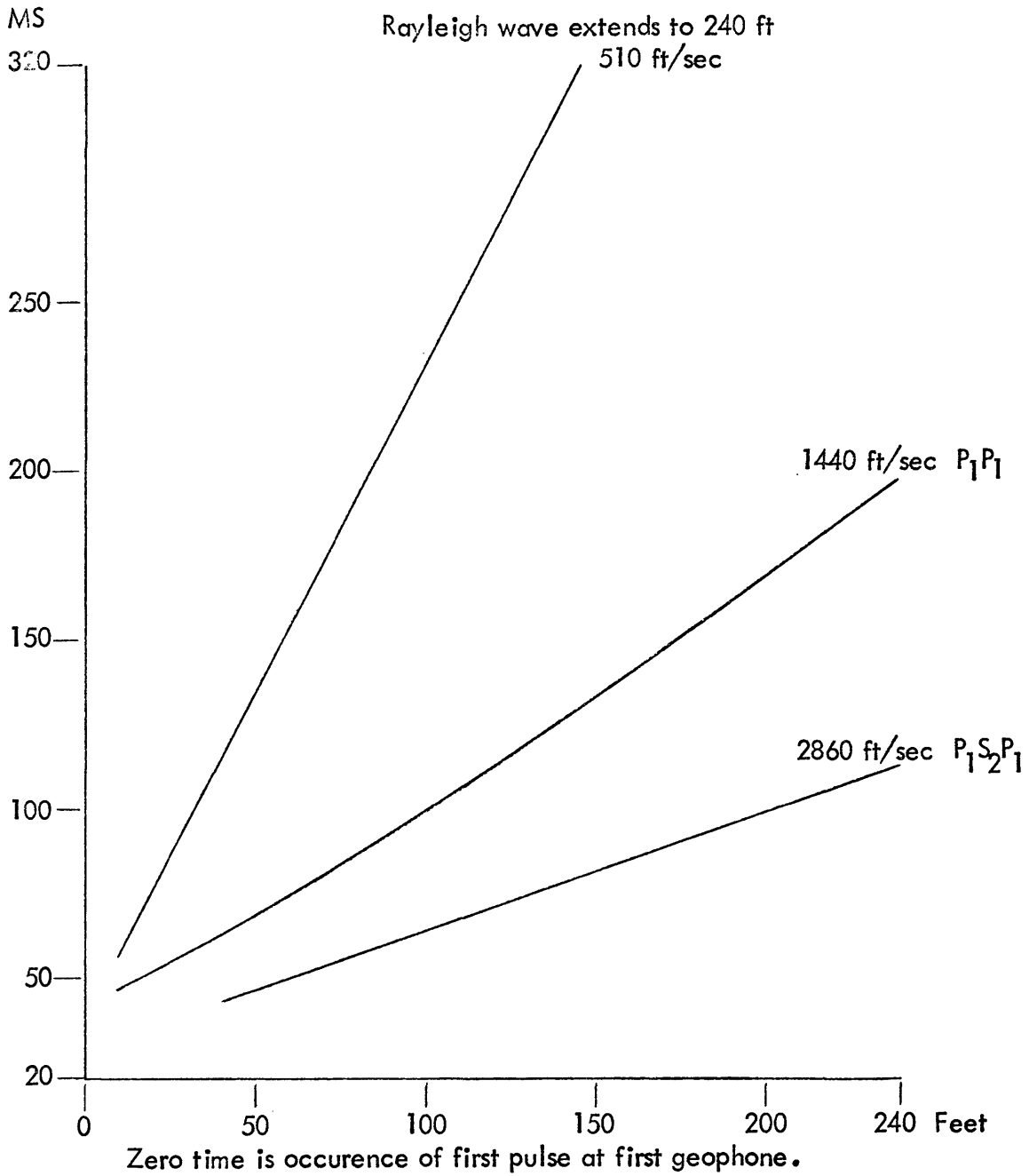


FIGURE 22. Time distance plot for surface and body waves at the Biddle Farm.

This is unusual since, McDonald's measurements were made at a much deeper level. The data from the Biddle Farm can be roughly compared with case 8 presented in Ewing and others (1957, p.207). The important ratios are calculated below.

$$\frac{\alpha_1}{\beta_1} = 2.62 \quad \frac{\beta_2}{\beta_1} = 5.21 \quad \frac{\mu_2}{\mu_1} = 27.1 \quad \frac{\rho_2}{\rho_1} = 1.0$$

For this case also, values of $2\pi/kH$ less than 0.65 imply that phase and group velocity are approximately equal and the Rayleigh velocity U is equal to $0.93 \beta_1$.

The results obtained from South Table Mountain are completely different than those obtained from the other areas. The location is a thick (approximately 100 feet) lava flow overlain by a few feet of unconsolidated material. The velocities found in the lava flow are higher, as might be expected. Figure 23 is a reproduction of one of the records obtained. The measured velocities are presented in Figure 24. There are four distinct velocities.

It is assumed that these velocities correspond to three different layers. As shown in Figure 25 it was possible to distinguish time delays due to refraction. The unconsolidated layer is rather thin and a thickness of 5 feet is assumed in the following.

In part due to the higher velocity and in part due to the thin layer, values of the parameter $2\pi/kH$ are substantially higher than previously encountered. The range is from 5.0 to 8.0. Examination of the theoretical Rayleigh curves in Ewing indicated that for this range of the parameter the

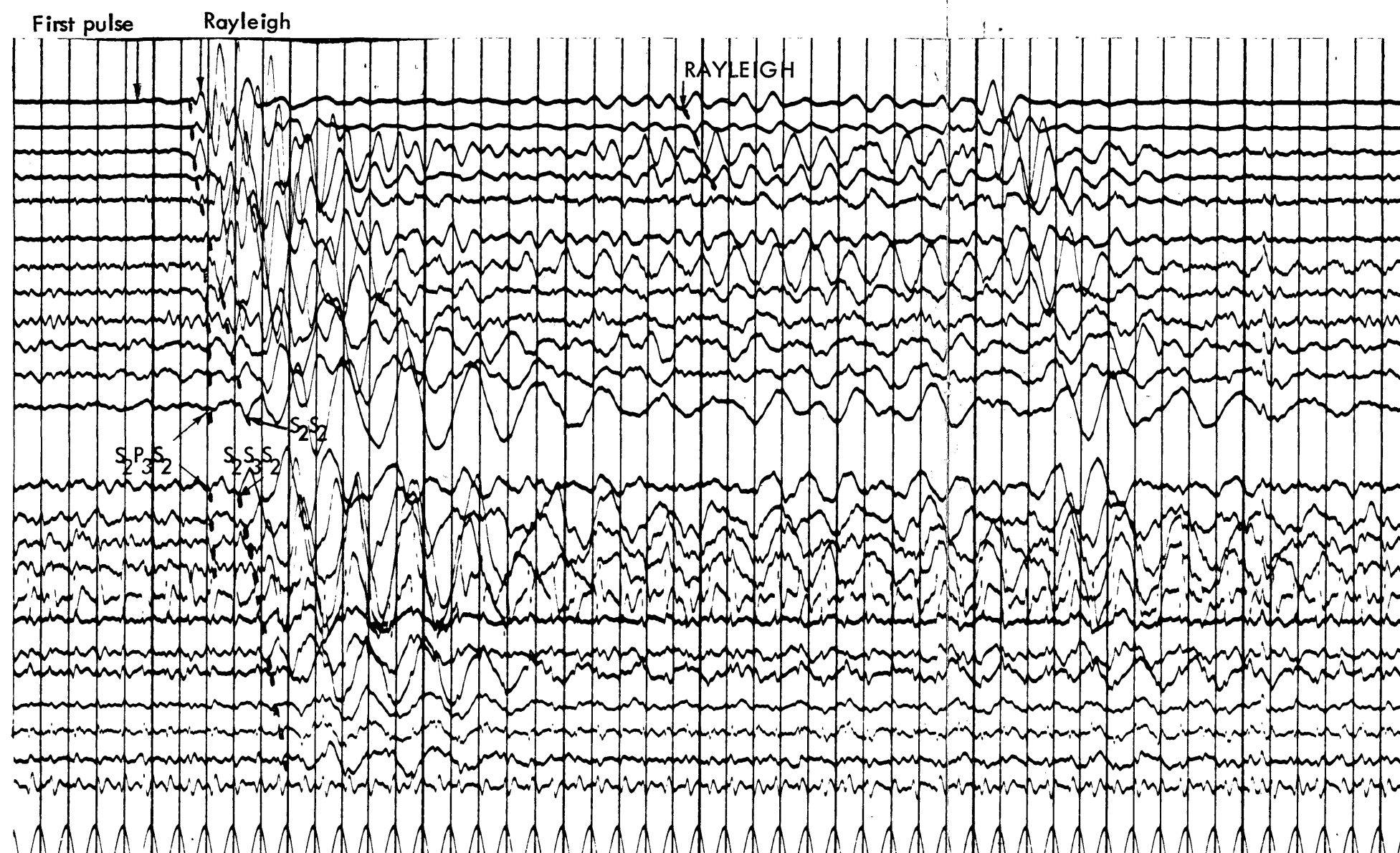


FIGURE 23. Field record from South Table Mountain.
 Run at 50Hz. Tape No. 353485
 High frequency filter at 120Hz
 Low frequency filter at 38Hz
 The first geophone is located 10 ft from vibrator.
 Geophone spacing 10 ft
 Each division is 10 ms
 Duration of run 376 ms

EVENT	CRITICAL DISTANCE :	VELOCITY
$S_2P_3S_2 (\alpha_3)$	59 ft	11030 ft/sec
$S_2S_3S_2 (\beta_3)$	157 ft	5840 ft/sec
$S_2S_2 (\beta_2)$		4480 ft/sec
RAYLEIGH		2960 ft/sec

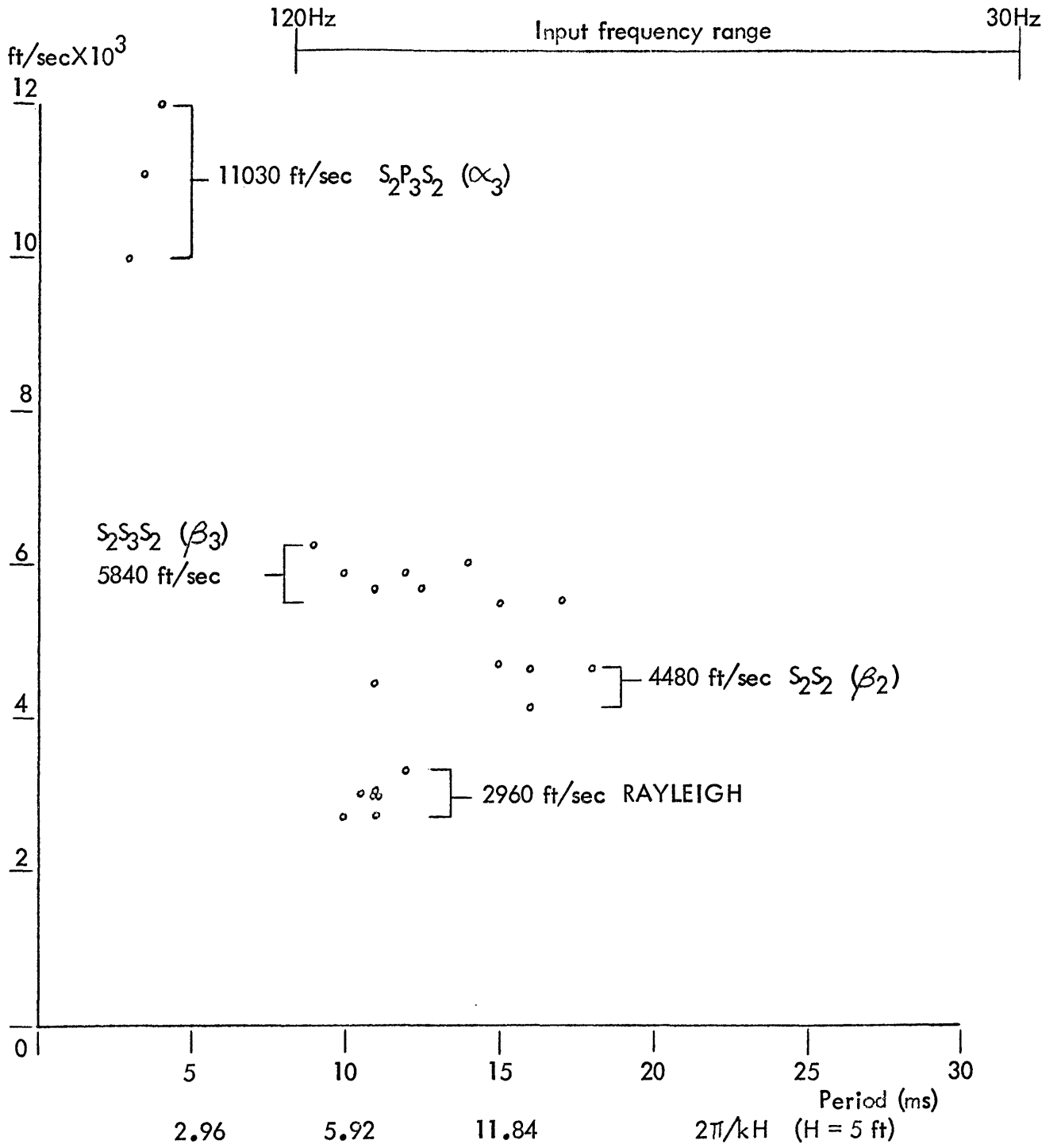


FIGURE 24. Average velocities South Table Mountain.

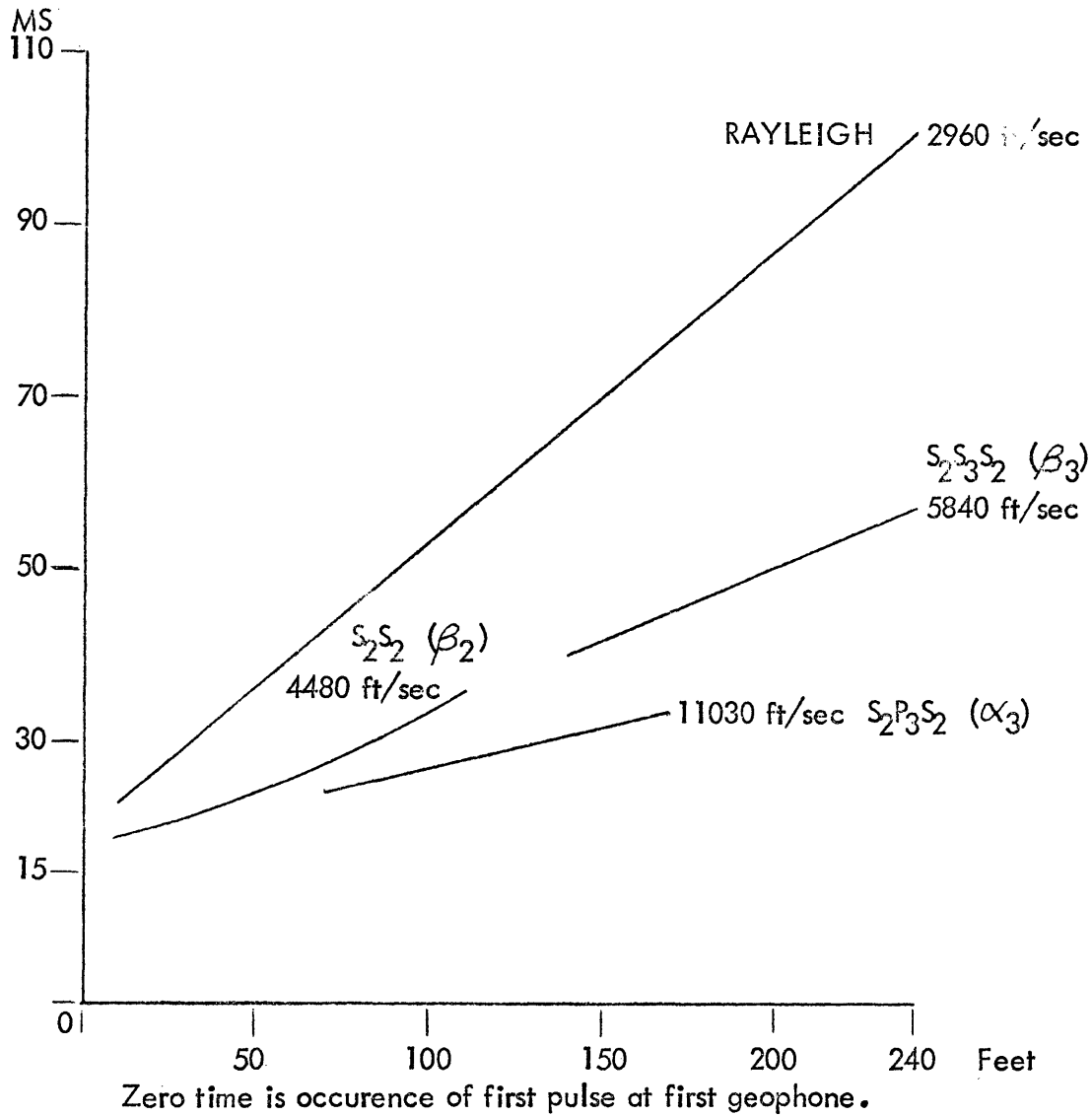


FIGURE 25. Time-distance plot for surface and body waves at South Table Mountain.

Rayleigh group velocity is larger than the upper layer shear velocity. The ratio of these velocities varies depending upon the earth characteristics.

In the range of 5.0 to 8.0 the ratio of U to β_1 rises rapidly, with lower values corresponding to lower values of $2\pi/kH$. This same trend is noticed on the measured velocities in Figure 24. While the inaccuracies of measurement prohibit a definite evaluation of this trend, certainly an opposite trend is not exhibited.

The 4480 ft/sec velocity grouping is interpreted as the shear velocity β_2 in the intermediate layer. The remaining two velocities can be interpreted as β_3 and α_3 . The Poisson's ratio for these two waves is 0.31. These two refractions are $S_2S_3S_2$ and $S_2P_3S_2$ and the layer thickness calculated from their velocities and intercept times are respectively 74 ft and 58 ft. Using the average thickness of 66 ft, the critical distances are 157 ft and 59 ft. The arrival time of the S_2S_2 reflection at 10 ft using the above values is 31 ms. The observed arrival time is 24 ms. This is allowing 5 ms for the time difference between vibrator start and the first pulse observed at the first geophone.

The main purpose of the field investigation was to show that the vibrator would produce interpretable data. The interpretation given above was selected on the basis of internal consistency. All other combinations of ray paths gave poorer fit to the data. No independent checks were made of the velocities and refractor depths using more conventional or direct techniques, for example, an uphole survey, two way refraction or core drilling.

CONCLUSIONS

The results of the field investigation have definitely indicated that the vibrator can be a useful tool in near-surface seismic exploration. In retrospect three features of the vibrator seem to be especially desirable. The first is the low cost and simplicity with which field records can be obtained. The second is the ease of reproducing input to the ground allowing careful alignment of amplifiers and elimination of automatic gain control. Third, the vibrator seems to be field-worthy and reliable.

The vibrator can be operated either horizontally or vertically and if desired it can be used as a single pulse source. For vertical operation it was found that upon starting and stopping the mass would hit the lower stop causing an unusually large pulse. This large pulse can be used as an impulse source.

In order to operate the vibrator over the complete range of frequencies the supply air pressure must be over 120 psig. All records made during the field investigations were made using 200 psig supply pressure. To take full advantage of this high pressure the modified sliding plate was used. This modified sliding plate has increased the power output as much as possible.

Throughout the interpretation of the records it has proved valuable to identify the Rayleigh wave. Any ambiguity in identification can

be removed in future field tests by using a combination of horizontal and vertical geophones.

For future work with the vibrator the previous field tests definitely indicate the need for an output at the vibrator to provide an accurate starting time. An accelerometer placed on or adjacent to the vibrator or the pressure gauge in the driving cylinder could accomplish this. This output could also be used as an input when the records are to be correlated.

Further field investigations should be carried out to determine the feasibility of applying the correlation technique to a portable field recording system. In addition the constant vibrator output is ideal for amplitude studies in refraction surveys. The generation of horizontally polarized shear waves with the vibrator operating horizontally could also form the basis for a useful field investigation.

REFERENCES

- Anderson, B.W., 1967, The analysis and design of pneumatic systems: New York, John Wiley & Sons, Inc., 303p.
- Anstey, N.A., 1966, Correlation techniques- A review: Jour. Can. Soc. Exp. Geophys., v.2, p.55-82.
- Blackburn, J.F., Reethof, G., and Shearer, J.L., 1960, Fluid power control: Cambridge, M.I.T. Press, 710p.
- Boothe, W.A., 1965, A lumped-parameter technique for predicting analog fluid amplifier dynamics: ISA Trans., v.4, p.84-92.
- Cagniard, L., 1962, Reflection and refraction of progressive seismic waves, translated by E.A. Flinn and C.H. Dix: New York, McGraw Hill, 282p.
- Cherry, J.T., and Waters, K.H., 1968, Shear-wave recording using continuous signal methods: Geophysics, v.33, p.229-239.
- Crane Co., Engineering Division, 1957, Flow of fluids through valves, fittings, and pipe: Chicago, Crane Industrial Products Group, Tech. paper no. 410.
- Crawford, J.M., Doty, W.E.N., and Lee, M.R., 1960, Continuous signal seismograph: Geophysics, v.25, p.95-105.
- Dobrin, M.B., Simon, R.F., and Lawrence, P.L., 1951, Rayleigh waves from small explosions: Am. Geophys. Union Trans., v.32, p. 822-832.
- Evison, F.F., 1953, An improved electromechanical seismic source tested in shattered rock: New Zealand J. Sci. Technol., v.35, p.4-13.
- Ewing, W.M., Jardetsky, W.S., and Press, F., 1957, Elastic waves in layered media: New York, McGraw Hill, 380p.
- Gill, M.S., and Thuren, J.B., 1966, Fluid amplifier state-of-the-art report: NASA Report on Contract NAS 8-5408, 27p.

- Howell, L.G., Kean, C.H., and Thompson, R.R., 1940, Propagation of elastic waves in the earth: *Geophysics*, v.5, p.1-14.
- Knox, W.A., 1967, Multilayer near-surface refraction computations, republished in *Seismic refraction prospecting*, edited by Musgrave, A.W.: Tulsa, Soc. Exp. Geophys., p.197.
- McDonal, F.J., Angona, F.A., Mills, R.L., Sengbush, R.L., Van Nostrand, R.G., and White, J.E., 1958, Attenuation of shear and compressional waves in Pierre Shale: *Geophysics*, v.23, p.421-439.
- Purseley, H., 1956, The power radiated by an electromechanical wave source: *Phys. Soc. (London) Proc. B*, v.69, p.139-144.
- Streeter, V.L., 1962, *Fluid mechanics*: New York, McGraw Hill, 555p.
- Townsend, R.W., 1965, Damping characteristics of a pneumatic dashpot: M.S. Thesis, Ariz. State Univ.

APPENDIX A
SUPPLEMENTARY FORMULAE

In this section will be found those equations which are necessary for calculations in the main parts of the thesis. These formulae are of sufficiently frequent usage that no derivations are necessary, only references will be given.

STEADY FLOW OF COMPRESSIBLE GASES THROUGH RESTRICTIONS

The steady flow of compressible gases through restrictions is described by the equation below (Anderson, 1967, p. 20).

$$W_{ud} = \frac{K P'_u A_{ud} N_{ud}}{\sqrt{T'_u}}$$

For the conditions of this study K is independent of pressure and temperature and has the constant value for air of $0.532 \sqrt{^\circ R/sec}$.

The factor N_{ud} is given by:

$$N_{ud} = \left[\frac{(P'_d/P'_u)^{2/\gamma} - (P'_d/P'_u)^{(\gamma+1)/\gamma}}{\left(\frac{\gamma-1}{\gamma}\right) \left(\frac{2}{\gamma+1}\right)^{(\gamma+1)/(\gamma-1)}} \right]^{1/2}$$

This factor is dependent upon pressure ratio and values for air are given in Appendix B .

A_{ud} is the effective area of the restriction and is obtained from the geometric area A by multiplying by the constant C . This constant has been determined experimentally for certain specific restriction geometries. In this thesis only square-edged and sharp-edged orifices are used. The discharge co-efficient C for the square edged orifice is 0.82. The discharge co-efficient for the sharp edged orifice varies as a function of pressure ratio. See Appendix C .

In applying the restriction flow formula the following points should be remembered.

1. P'_u is total pressure upstream of restriction and this can only be equated to upstream static pressure if upstream velocity is low.
2. P'_d is total downstream pressure and can be equated to downstream static pressure only if downstream pressure recovery is low. In effect, this means that no abrupt pressure increase takes place immediately downstream from the orifice.

GENERAL GAS LAW

This form of the gas law conveniently relates mass, pressure, volume and temperature of a gas. For all conditions encountered in this thesis air behaves as an ideal gas of molecular mass 29.0.

$$P' V' = mR' T'/M$$

APPENDIX B

TABLE OF VALUES FOR RESTRICTION FLOW CALCULATIONSValues of N_{Ud} for $\gamma = 1.40$ (air)

P'_u / P'_d	N_{Ud}
1.0000	0.0000
1.0010	0.0652
1.0025	0.1030
1.0050	0.1453
1.010	0.2044
1.025	0.3183
1.050	0.4390
1.10	0.5916
1.20	0.7642
1.30	0.8609
1.40	0.9199
1.50	0.9566
1.60	0.9791
1.70	0.9920
1.80	0.9984
1.90	1.0000

APPENDIX C

VALUES OF CONSTANT FOR SHARP-EDGED ORIFICE FLOW CALCULATIONS

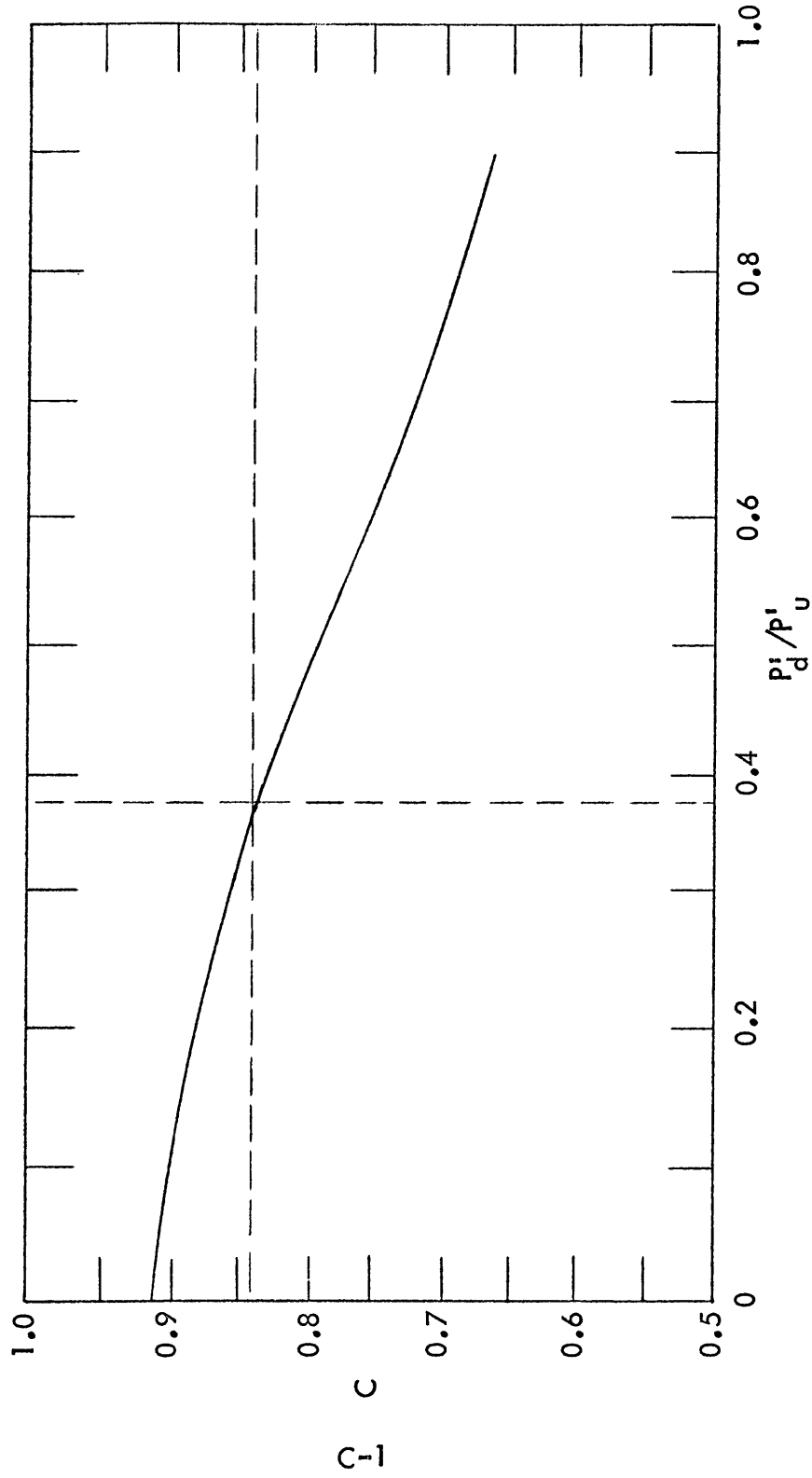
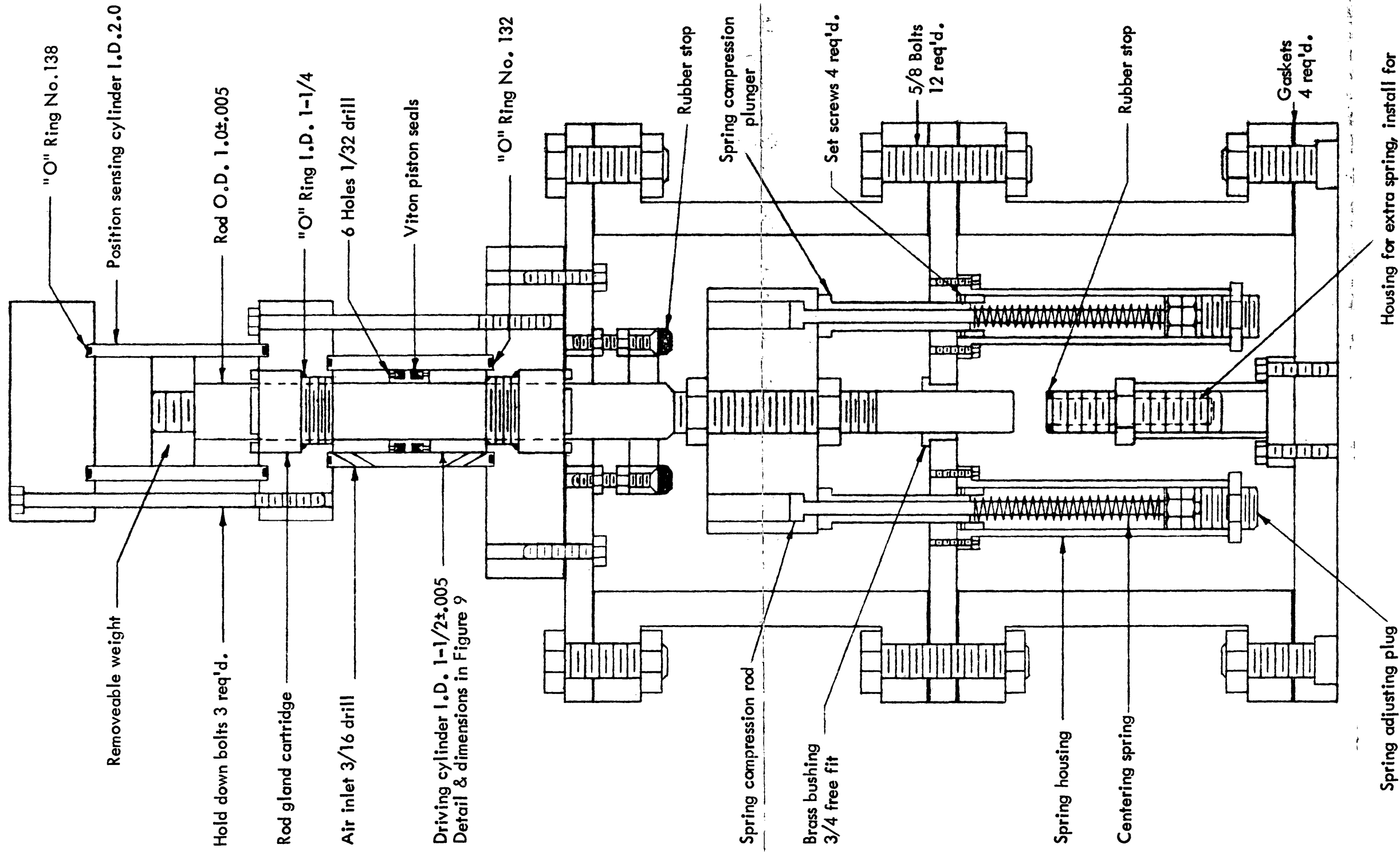


FIGURE C-1. Sharp-edged orifice data (from Anderson, 1967, p. 32).



Housing for extra spring, install for vertical operation and remove for horizontal operation.

SCALE MISSING DIMENSIONS
Scale 1/2"=1"

Rod gland cartridge: Parker Hannifin RG2AHL-105
Viton piston seals: Parker Hannifin PK1502A005

APPENDIX D
FIGURE D-1. Assembly drawing of vibrator.

APPENDIX E

BIBLIOGRAPHYAnalysis and Design of Fluidic Components

- Adam, R. B., 1965, Application of fluidic valves: A S M E paper 65 WA/PID-12.
- Aizerman, M. A., 1965, Pneumatic and hydraulic automation: DDC Report AD-618061.
- Bauer, P., 1965, Binary counter stages having two vortex amplifiers: U. S. Patent No. 3,193,197.
- Bjornsen, B. G., 1964, The impact modulator: Proc. HDL Fluid Amplification Symposium, v.2.
- Bowles, R. E., and Dexter, E. M., 1965, A second generation of fluid system application: Proc. 3rd. HDL Fluid Amplification Symposium, v.3.
- Cargill, N. A., and Reader, T. D., 1964, Electro-sonic fluid amplifier: U. S. Patent No, 3,144,037.
- Carter, V., and Fine, J., 1964, Fluid amplification technology: A bibliography of direct contributions: Proc. 2nd HDL Fluid Amplification Symposium, v.3.
- Carwile, C. L., 1962, An analytical and experimental study of the pressure of a small chamber to forced pressure oscillations: Princeton University Aero. Eng. Report No. 595d.
- Duff, J., Foster, K., and Mitchell, D. G., 1965, Some experiments on the vortex valve: Cranfield, England, First Conf. Fluid Logic and Amplification, Brit. Hydromech. Res. Assoc.
- Gordon, M. H., 1965, Design, fabrication and test of a fluid interaction servo-valve: NASA Report on contract NAS 3-5212.
- Greber, I., Koerper, P. E., and Taft, C. K., 1965, Fluid vortex amplifier optimization: Proc. HDL Fluid Amplification Symposium, v.2.

Harvey, D. W., and McRae, R. P., 1965, Experimental study of fluid controlled valves: Proc. 3rd HDL Fluid Amplification Symposium, v.4.

Howland, G. R., 1965, Performance characteristics of vortex amplifiers: Proc. HDL Fluid Amplification Symposium, v.2.

Lansky, Z. J., 1965, Practical guides to pneumatic valve application: Automation, p. 61.

MIT, Dept of Mech. Eng., 1965, Basic applied research in fluid power control: Report No. 8998-2 on Contract AF33 (657-7535).

Mayer, E. A., and Maker, P., 1964, Control characteristics of vortex valves: Proc. 2nd HDL Fluid Amplification Symposium, v.2.

Otsap, B. A., 1964, Experimental study of a proportional vortex fluid amplifier: Proc. HDL Fluid Amplification Symposium, v.2.

Rivard, J. G., and Walberer, J. G., 1965, A fluid state vortex hydraulic servovalve: Chicago, 21st. National Conf. Fluid Power.

Roffman, G. L., 1964, Staging of closed proportional fluid amplifiers: Proc. 2nd. HDL Fluid Amplification Symposium, v.3.

Taft, C. K., and MacLaughlin, D. W., 1967, Fluidic electrofluid converter: Jour. Basic Eng., v.89, p. 334-340.